HOMOGENEOUS CATALYSIS
DEVELOPMENTS IN THE SYNTHESIS OF ZWITTERIONIC OLEFIN POLYMERIZATION CATALYSTS AND IRON CONTAINING CATALYSTS FOR HYDROCARBON OXIDATION

By

GARRY KENNETH WEAKLEY

A DISSERTATION PRESENTED TO THE GRADUATE SCHOOL
OF THE UNIVERSITY OF FLORIDA IN PARTIAL FULFILLMENT
OF THE REQUIREMENTS FOR THE DEGREE OF
DOCTOR OF PHILOSOPHY

UNIVERSITY OF FLORIDA

2003

TABLE OF CONTENTS

ACKNOWLEDGMENTS

The individuals deserving thanks from the author for their role in the completion of this dissertation are many. First and foremost, I would like to thank my parents, Garry and Judy, for their guidance and support through this long and enduring process. Because of them, I am who I am today, and their love and guidance have helped me be successful not only in chemistry, but in life as well. I also want to thank my wife Cherry for her unquestionable loyalty and support to our family and myself. I was blessed during my stay in Gainesville by the birth of my son Jordan. Cherry has been a constant source of strength and motivation throughout this process, and was not only a good wife and companion to me, but also a good mother to Jordan. Having a loving family during graduate school gave me a very good distraction from the problems at school, and for that I am extremely grateful.

My most sincere respect and gratitude are extended to my research advisor, Dr. David E. Richardson, for his support and guidance through the past five years. His advice and encouragement during some of the most difficult times of my research and his enthusiasm over the few successes have been a constant source of motivation. Most importantly, he has shown me the importance of understanding the fundamentals, whether it relates to chemistry or life.

I also wish to thank Dr. James M. Boncella for the leadership and guidance through the difficult synthesis of the anions. Most importantly, Jim taught me everything

I know about working with air and moisture sensitive chemicals, without which most of this dissertation would not have been successful Jim became a good friend during the five years in Florida, through the group meetings at the golf course and the evenings at the softball field (even though I pushed him in the mud at home plate), for that I truly appreciate him

There were many people that passed through the Richardson and the Boncella groups during my stay here I need to thank each and every one, for they all have played an important role in the completion of this dissertation Special thanks goes to Dr Joy Mendez, Dr Jerrold Miller Dr Celeste Regino, Dr Deon Bennett Dr Carlos Ortiz, Anna Ison, Dan Donevan and Andy Burke for being great friends as well as coworkers.

Thanks also go to Ryan Mills for being a constant source of friendship during these five years This is greatly appreciated because many problems about chemistry and life were discussed over a few drinks at the Porpoise and the Dog I would also like to thank all of the friends that I have made in my time in Gainesville. Each and every one of them played an important role and will always be remembered Without them, any resemblance of normal life would have been impossible.

Abstract of Dissertation Presented to the Graduate School
of the University of Florida in Partial Fulfillment of the
Requirements for the Degree of Doctor of Philosophy

HOMOGENEOUS CATALYSIS
DEVELOPMENTS IN THE SYNTHESIS OF ZWITTERIONIC OLEFIN
POLYMERIZATION CATALYSTS AND IRON CONTAINING CATALYSTS
FOR HYDROCARBON OXIDATION

By

Garry Kenneth Weakley

May 2003

Chairman: David E. Richardson
Major Department: Chemistry

Cationic 14-electron metal-alkyl complexes $[(\eta_5\text{-}\ C_5H_3)_2M\text{-}R]^+$ (M= Ti, Zr, Hf) have been established as the active species in homogeneous polymerization of olefins. Our research interests have focused on gaining some control over ion pairing between the metal cation and its anion, by covalently linking a borate anion to the ligand backbone of the transition metal complex. One approach to accomplishing this goal is to prepare a zwitterion, where the charges are physically separated by covalently linking the borate counterion to the ligand backbone of the catalyst. Our methods involve the building of a robust B-C bond that will remain intact during the polymerization process. The reaction of $Li_2[(CH_3)_4C_5(SiCH_3)_2(p\text{-}C_6F_4\text{-}B(C_6F_5)_2]$, ($Li_2[Cp^B]$) with $(C_5H_5)ZrCl_3$ produces an anionic sandwich complex $Li[(C_5H_5)(Cp^E)ZrCl_2]$. This complex is an active ethylene polymerization catalyst once activated with MAO. The preparation of ligands and the X-ray crystal structure of an anionic metallocene $Li[ZrCl_2(C_5H_5)\text{-}(C_5(CH_3)_4\text{-}Si(CH_3)_2\text{-}C_6F_4\text{-}p\text{-}B(C_6F_5)_3]\ \ 2(i\text{-}Pr_2O)$ are discussed.

Catalytic oxidation of hydrocarbons can be accomplished by employing homogeneous iron salts. One substrate of particular interest is cyclohexane and its higher oxidation products cyclohexanol (A) and cyclohexanone (K). We have developed a system in which the oxidation of cyclohexane can be accomplished by the addition of Iron (II) or Iron (III) salts in neat cyclohexane solution under mild conditions. The system development and optimization of the process is discussed.

CHAPTER 1

THE ROLE OF CATALYSTS IN CHEMISTRY

Introduction

A catalyst is defined as a substance that accelerates the rate of a chemical reaction or process without being consumed in the reaction. Generally, a catalyst makes available reaction pathways that are kinetically more favorable and have lower activation energies than the corresponding uncatalyzed reactions.[1] Activation energies of such reactions are often lowered by the interaction of the catalyst with the substrate, which provides an alternate mechanistic pathway. This alternate pathway permits reactions or processes to proceed more efficiently or under milder conditions than would otherwise be possible.

The form of a catalyst can vary dramatically from a simple organic acid or base to complex organometallic species. Organometallic species are of particular importance due to their broad applications in catalysis. Organometallic complexes have been the focus of intense research due to its applications in catalysis of hydrocarbon oxidation, olefin polymerization, hydrogenation, as well as numerous other organic transformations.[2-4] Organometallic complexes can function in either a homogeneous or heterogeneous reaction medium. Heterogeneous catalysis currently dominates industrial chemical production in terms of volume of product produced, but homogeneous

catalysis is gaining acceptance in industry due to the unique properties offered by the catalytic organometallic complexes

The broad applications of organometallic species are in part due to the diversity of the transition metal series. Changing the metal center of the organometallic complex can dramatically alter the properties of the catalytic species. Electronegativity of the transition elements increase significantly going from left to right across the periodic table. Early transition metals are electropositive and are commonly found in higher oxidation states. This means that the valence electrons of the early transition metals reside in high energy molecular orbitals and are readily lost. Thus, the d^0 metals are very Lewis acidic and are able to bind unsaturated ligands strongly.

Alternatively, the middle and late transition metals are relatively electronegative and are commonly found in lower oxidation states. This is a result of the molecular orbitals residing at lower energy levels, which make the lower oxidation states more stable. Late transition metal complexes that have high oxidation states often find ways of attaining lower more stable oxidation states. As a result, these metals bind unsaturated ligands and make them susceptible to nucleophilic attack by placing positive character on the ligand due to its limited back donation properties. This difference in the electronegativity among the transition metal series and different ligand environments gives rise to a wide range of reactivity in catalysis.

Essential characteristics of a catalytic reaction are the same whether the catalyst is soluble or insoluble. Generally there are three basic characteristics that apply: (1) the effect of the catalyst is purely kinetic. It does not make a thermodynamically forbidden reaction available, but it can dramatically accelerate a thermodynamically allowed

reaction by providing a pathway that has a lower energy of activation (2) Catalytic reactions operate in a cyclic fashion through a series of reactions that are repeated each time a molecule of the substrate is transformed (3) The active catalytic species is not necessarily the same compound that is added to the reaction mixture Many transformations of the catalyst usually occur in order to activate the catalyst These pre-catalytic reactions often give rise to an induction period before catalysis begins.

Catalysis of organic reactions by soluble transition metal complexes has become a major synthetic tool both in the academic laboratory and in industrial chemical production Organometallic chemistry merged the fields of organic and inorganic chemistry by examining the interaction between metal ions and organic molecules Wilkinson,[5,6] Fischer,[7-10] Ziegler,[11,12] and Natta[13,14] provided the basis for organometallic chemistry[3] and homogeneous catalysis as we know it today, and each has received a Noble Prize for his contribution

Homogeneous Catalysts

Homogeneous catalysis has experienced major growth in the last four decades [15-17] This growth is due to the unique selectivity and tunability of organometallic complexes, which have allowed for the development of new products with unique properties that today's consumer demands The industrial application of homogeneous catalysis has led to a greater understanding of the chemistry involved. Mechanistic studies typically follow commercial application, but the information from these studies has been valuable for the optimization of reaction conditions and in the development of new catalysts Mechanistic studies of homogeneous catalysis has

rapidly advanced due in large part to the physical organic spectroscopic techniques that can be applied to these systems with little or no modification. Many of the mechanistic principles developed from homogeneous reaction investigations can be applied to heterogeneous systems for which much less mechanistic information is available.[18]

Small changes made to the structure or electronic properties of the catalyst can have a significant impact on its activity and selectivity. Reaction rate optimization and catalyst selectivity can be adjusted by manipulating the steric and electronic properties of the ligand and the metal center. Seemingly unlimited structural variation of organic ligands and a diverse range of metals result in a wide range of catalyst variations, generating catalysts with greater selectivity and reactivity control in most reaction mediums. Incorporating various functional groups on the metal complex allows one to change the solubility of the metal complex so it can be employed in a variety of different solvents. Ligand design can selectively modify the reactive site resulting in greater selectivity toward different substrates and even asymmetric catalysis.

Selectivity, high yields, product purity, and the ability to operate under mild conditions of temperature and pressure are the major virtues of homogeneous catalysis that has led to its current expansion in industrial applications. These characteristics are especially important in the pharmaceutical and polymer industries, where intermediates and products must be extremely pure.

Fundamental Reactions

Due to the enormous volume of literature regarding the applications of homogeneous catalysis, this chapter will not attempt to review the literature, but it will highlight the flexibility of several homogeneous catalysts and their properties. Major

reaction pathways in homogeneous catalysis are simply fundamental reactions of coordination and organometallic chemistry. Reactions appear in many combinations and sequences in catalytic cycles and in the activation of catalyst precursors. Fundamental reactions include ligand association and dissociation, oxidation / reduction, oxidative addition / reductive elimination, and insertion / elimination. A brief overview of the fundamental reactions will also be discussed in this chapter. A detailed discussion involving oxidation and insertion reactions are reserved for the chapters where they have the most relevance to this dissertation.

Oxidation / Reduction

Catalytic oxidations of organic substrates by soluble metal complexes represent a very important class of catalysis. The metal ion in these oxidation-reduction reactions commonly cycle between two stable oxidation states. Homogeneous cyclohexane oxidation, in particular, involves a cobalt ion cycling between the +2 and +3 oxidation states. The catalytic complex does not interact with either the O_2 or hydrocarbons, instead the major function of the catalyst is decomposition of organic peroxides. The organic peroxide is formed spontaneously, by reaction of the hydrocarbon with O_2 (autoxidation), and then is decomposed by the metal complex, leading to the production of free radicals. The resulting free radicals carry the autoxidation propagation reactions. The metal catalysts used for this peroxide decomposition usually employ the readily available, hydrocarbon-soluble salts such as naphthenates and acetate ligands.

$$ROOH + M^{+2} \longrightarrow RO^{\cdot} + HO^{-} + M^{+3} \quad (1)$$

$$ROOH + M^{+3} \longrightarrow ROO^{\cdot} + H^{+} + M^{+2} \quad (2)$$

Figure 1-1 Metal catalyzed peroxide decomposition

Oxidative addition / Reductive elimination

In addition to conventional oxidation and reduction reactions, another important reaction class in catalysis is oxidative addition / reductive elimination. This class of reactions are central to important industrial processes such as hydroformylation and hydrogenation.[18,19] The most common catalysts used for these transformations are low valent group 8-10 transition metals.[3] Low valency is necessary in order to supply sufficient electron density to facilitate the interaction with the CO and/or H_2 ligands. Transition metal complexes utilize d orbitals as well as symmetry of the catalytic complex to assist the metal-ligand binding. The important interactions for metal catalysis exist in the coordinate bonds between a neutral ligand and the metal center. The symmetries of the orbitals involved in the coordinate bonds are very important to the stability of the bond. Figure 1-2 illustrates how the CO Highest occupied molecular orbital (HOMO) donates electrons to the metals Lowest unoccupied molecular orbital (LUMO), the empty $M(d_{z^2})$ orbital, while the metal HOMO, filled $M(d_{\pi})$ orbital, back donates to the CO LUMO. This back donation polarizes the CO bond, which in turn chemically activates the CO.

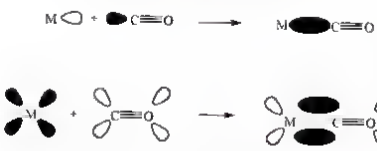

Figure 1-2. MO bonding model for M-CO interactions

The ligands of the catalyst can have significant influence on the binding properties of the metal catalyst Ligands must be appropriately fit to the catalyst to permit the desired organic transformation and to complete and support the catalytic cycle In the case of hydroformylation by a rhodium catalyst,[20] phosphine ligands offer the appropriate environment, both sterically and electronically, for the reaction to proceed selectively and efficiently Use of this rhodium catalyst allowed Wilkinson et. al [21-25] to propose the mechanism in Figure 1-3 Mechanistically this catalytic reaction encompasses some of the fundamental reactions available i e., coordination of an olefin, insertion of CO, oxidative addition of H_2, and reductive elimination

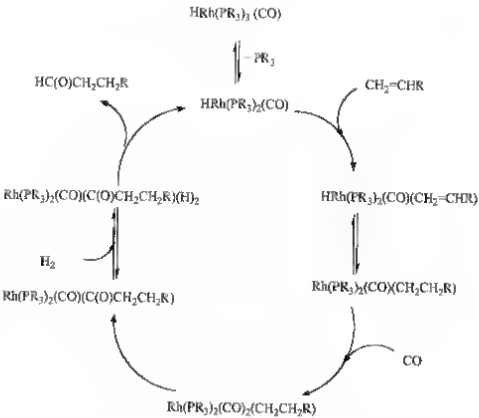

Figure 1-3 Wilkinson's Hydroformylation Catalytic Cycle[23]

Hydrogenation reactions are akin to hydroformylation with the exception of the CO insertion step. A good example of a hydrogenation catalyst that is used in the production of asymmetric diamines is the Rh(I) catalyst developed by Dupont[26] that can catalyze the asymmetric hydrogenation of enol acetates to 100 % yield and up to 99% ee. High ee's and yield can be accomplished by incorporating the appropriate asymmetric phosphines ligand onto the rhodium catalyst (Figure 1-4). Simply changing the ligand of the catalyst to the R,R ligand configuration will produce the R product isomer, and changing the ligand conformation to the S,S configuration will produce the

S product isomer (Figure 1 5) This is just one example of the powerful synthetic utility of homogeneous catalysis that is not easily obtained from a heterogeneous catalyst

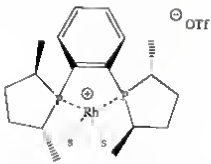

Figure 1-4 [R,R]-DuPhos Rh(I)

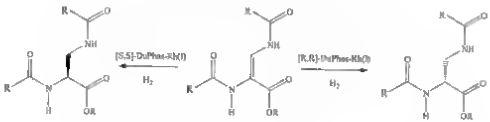

Figure 1-5. Asymmetric hydrogenation of α,β Diamidopropenoates[26]

Insertion / Elimination

Insertion and elimination are fundamental reactions that are ubiquitous to the catalytic chemistry of olefins A prime example of this reaction category is the insertion of an olefin into a metal-alkyl bond.

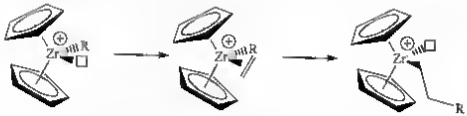

Figure 1-6 Insertion of an olefin into a metal alkyl bond

The term insertion is a useful description of the overall reaction, but is inaccurate in mechanistic detail. A better description of the overall reaction is migration of an alkyl or hydride ligand from the metal center to the carbon of the coordinated olefin. Two steps are involved in insertion reactions: olefin coordination and carbon-carbon (or carbon-hydrogen) bond formation. In all well-characterized insertion reactions the unsaturated substrate (olefin, diene, CO, etc.) is coordinated to an open coordination site cis to the migrating ligand of the metal atom. The second stage incorporates the migration of the alkyl bond to the coordinated olefinic substrate.

The overall rate of the second step is important in controlling the molecular weight of the polymer, when multiple insertions occur the length of the polymer increases. For high molecular weight polymers the propagation rate is rapid[27] compared to the termination rate. The major termination pathway for these types of reactions involves β-elimination,[28] in which a hydrogen on the β carbon of the polymer chain is transferred to the metal center resulting in a metal hydride bond and a coordinated olefin. The coordinated olefin can then either re-insert the hydrogen, which can result in branching, or get displaced by the monomer to start a new polymer chain.

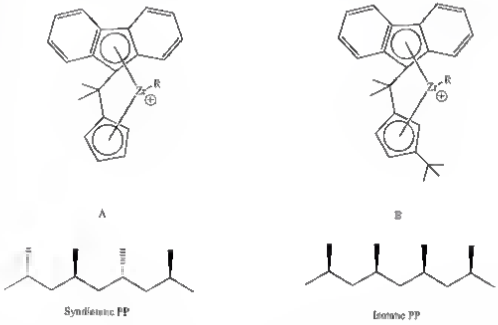

Figure 1-7. β-hydrogen elimination and reinsertion

Catalysts used for olefin polymerization incorporate a broad range of transition metals from group 4 through group 10. Most often the active catalysts are 14-electron cationic species that have a wide range of ligand and metal variations. A plethora of structural variations coupled with the wide range of metals available allows for the polymer properties to be tailored to fit specific needs. A good example of this catalyst tailoring can be illustrated by the polymerization of propylene[29,30] where making minor changes in the catalyst structure will produce polypropylene with different tacticity

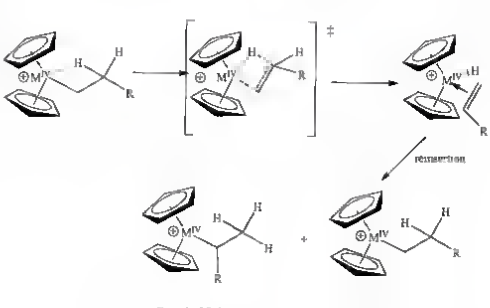

Figure 1-8 Syndotatic and Isospecific Metallocene Catalysts

Figure 1-8 shows that by substituting one position of the Cp ring can produce isotatic polypropylene where the unsubstituted Cp ring produces the syndotactic polypropylene [31] The key to these types of catalysts is that the steric bulk of the ligand directs the incoming monomer to obtain a certain orientation resulting in the desired tacticity of the polypropylene

The examples of homogeneous catalysis described above are not by any means an exhaustive representation of catalysis related to soluble organometallic complexes Several additional examples of this type of catalysis could be cited, for example, catalytic hydrosilylation [32-35] olefin isomerization,[22,36,37] and hydrocyanation,

[38-40] these examples clearly demonstrate the broad applicability that organometallic chemistry has in homogeneous catalysis

In this dissertation, the author's research regarding different types catalysts for two of the fundamental reactions, oxidation and polymerization, is presented. These discussions include the detailed attempts to create suitable anionic ligands for a zirconium polymerization catalyst in order to achieve a greater understanding of the chemistry involved in the catalytic polymerization process. The oxidation chemistry discussed involves the investigation of a hydrocarbon oxidation system catalyzed by soluble iron catalysts. Ligand structure and electronic properties of the iron catalyst were manipulated in order to achieve an efficient catalyst for the oxidation of cyclohexane.

Chapter 2

SYNTHESIS OF A METALLOCENE CONTAINING A LINKED PERFLUOROPHENYLBORATE FOR THE USE AS A ZWITTERIONIC OLEFIN POLYMERIZATION CATALYST

Introduction

In 1953 Karl Ziegler and coworkers, while at the Max-Planck Institute discovered that the combination of group 4 metal chlorides and triethylaluminium produced a catalyst that would polymerize ethylene at ambient temperatures.[41] This discovery was monumental considering that before this discovery polyethylene was produced by a radical mechanism that required extremely high temperatures and pressures. It was quickly realized that the most active catalytic system consisted of a combination of titanium tetrachloride and diethylaluminumchloride. The combination of the reagents produces fibrous $TiCl_3$ crystals that will catalyze the polymerization of ethylene efficiently. Following the work of Ziegler, Natta and coworkers[42] were able to demonstrate that an appropriate catalyst mixture was capable of polymerizing propylene into semi-crystalline polypropylene. The Noble prize in chemistry was awarded to both Ziegler and Natta in 1963 for their discoveries.

While the potential of the Ziegler and Natta discoveries was being realized, Wilkinson[43-45] and Fischer[46] were studying the structure and synthesis of metallocenes (also called sandwich compounds), where a π bonded metal atom is bound between two aromatic rings. Wilkinson and Birmingham[43] then later reported in 1954 the synthesis

of a series of group 4 metallocene halides as well as other transition metal metallocene complexes. The series included Cp_2TiCl_2 and Cp_2ZrCl_2 (Figure 2-1), which were later found by Breslow and Newberg[47,48] to be effective polymerization catalysts when activated with an aluminium cocatalyst. These metallocene complexes when mixed with diethylaluminumchloride polymerized ethylene to high molecular weight. The Breslow and Newburg study provided the tools needed for a detailed mechanistic investigation of the polymerization reaction.

Figure 2-1 Titanium and Zirconium metallocene complexes

Metallocene catalysts have several advantages: they are soluble in hydrocarbon solvents, provide a single reactive site, and their chemical structure can be easily manipulated. The single site nature of the metallocene complexes has allowed researchers to examine the effects that structure and reaction conditions have on the polymerization mechanism.[49-54] The catalytic activity of the metallocene system with the conventional alkylaluminium co-catalyst is about 10-100 times greater than the heterogeneous Ziegler-Natta systems. The authors also observed that the activity and molecular weight of the polymer was independent of the ratio between the catalyst and the co-catalyst, and independent of the type of alkylaluminium chloride reagent used. Trimethylaluminium was found to have little reactivity under the experimental conditions employed by Breslow and Newberg.[48] The exceptional reactivity of

trimethylaluminum wasn t realized until Sinn and coworkers[53] discovered that the presence of small amounts of impurities like water and oxygen significantly increased the rate of polymerization.[56,57] The research by Sinn and coworkers found that the impurities react with trialkylaluminum to form oligomeric aluminoxanes, which have a general formula $[RAlO]_n$ The most common aluminoxane is methylaluminoxane (MAO), the hydrolysis product of trimethylaluminum. MAO can be best described as a mixture of linear and cyclic oligomers that exist in equilibrium Barron has described MAO as a complex system of cross-linked cages[58,59] and linear species with the general structure shown in Figure 2-2 Metallocenes in combination with MAO produce an extremely active polymerization catalyst with rate enhancements observed 10 000-fold[55] greater than the traditional Ziegler-Natta system The zirconium complex, Cp_2ZrCl_2 when treated with MAO produces an ethylene polymerization catalyst capable of producing 1500 kg of PE per gram of catalyst per hour [53]

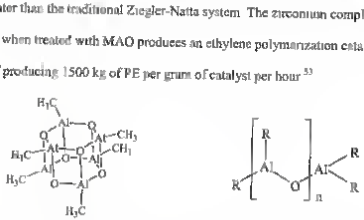

Figure 2-2 Generalized structure of MAO

Three steps are responsible for polymerization initiation, propagation, and termination (Figure 2-3) The initiation step involves the generation of an unsaturated metal alkyl complex Generation of the unsaturated metal complex can be achieved with strong Lewis acids, such as AlR_2Cl, MAO BR_3, etc Aluminium reagents alkylate the metallocene dichloride as well as abstract an alkyl ligand from the metal center to

generate the active catalyst. It is generally accepted that the active catalyst is a cationic transition metal alkyl complex

Olefin Polymerization Mechanism

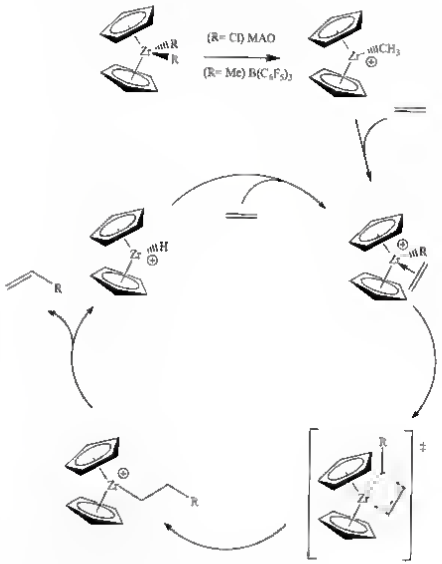

Figure 2-3 Cossee's proposed olefin polymerization mechanism by metallocene catalyst [68]

Propagation occurs in two steps: olefin coordination and carbon-carbon bond formation. Olefin coordination requires an open coordination site cis to the migrating alkyl ligand. The coordinating ability of the olefin determines the effectiveness of the polymerization for a given catalyst. The utility of this type of catalyst is limited to the simple unhindered terminal alkenes (rates of polymerization typically decrease in this order: ethylene > propylene >> 1-butene). Internal olefins are not usually polymerized by this type of catalyst due to the sterically limited coordination pocket of the metal center, and the resulting decreased coordinating ability of the higher olefin. Carbon-carbon bond formation is the second stage of the propagation process, and has been the subject of controversy in the scientific community. Cossee[61,62] and Green[63] developed mechanisms that have been accepted as the best possibilities for the polymerization mechanism. Cossee's approach suggests that the C-C bond-forming step goes through a four member transition state (Figure 2-3). Green and Rooney[63] suggested that the mechanism goes through a carbene hydride intermediate. Green and Rooney's proposal suggests that the alkyl chain eliminates a α-hydrogen producing a carbene hydride intermediate, which then inserts ethylene through a similar four-member transition state. The metallacycle intermediate then reductively eliminates producing an unsaturated metal alkyl complex (Figure 2-4). The carbene hydride mechanism cannot be applied to d^0 or d^1 metal complexes because the alkylidene hydride complex exceeds the permitted oxidation state for group IV metals. Considering that most common single-site polymerization catalysts are d^0 zirconium and titanium complexes, a modified Green Rooney mechanism was established. The modified Green Rooney mechanism replaced

the carbene hydride complex by an agostic alkyl hydride (Figure 2-5), which kept the oxidation state constant. It is important to note that for a different catalyst or catalyst system, either mechanistic pathway might prevail.

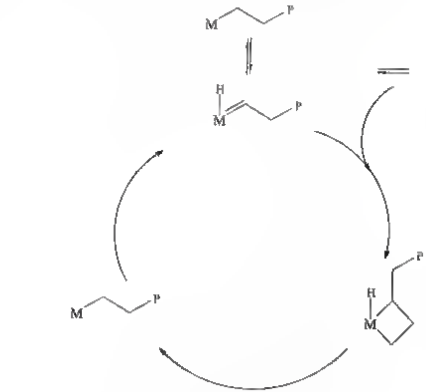

Figure 2-4. Carbene to metallocycle mechanism[60]

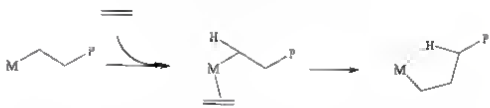

Figure 2-5. Modified Green Rooney Mechanism[65]

Termination is the final stage of the polymerization mechanism, and several possibilities exist.[64] The simplest and most straightforward chain terminating step is β-

Hydride elimination which is generally accepted to be the main mode of elimination,[65,66] β-Hydrogen elimination occurs through a four-center transition state where the metal-alkyl bond is broken while a metal-hydride bond is formed, from the β-hydrogen of the growing polymer simultaneously The product of the β-Hydride elimination is a cationic metal hydride and a coordinated terminal olefin. Two possible reinsertion modes exist for the metal hydride complex (1) the resulting olefin is displaced by a smaller more basic monomer (Figure 2-6) to start a new polymer chain (2) the olefin reinserts into the metal hydrogen bond either reforming the straight chain polymer or a branched polymer An alternative chain terminating reaction is the hydrogenolysis of the metal-carbon bond by the addition of hydrogen to the system. The products of hydrogenolysis are a saturated polymer and a metal-hydride complex Hydrogenolysis is mainly used to control the molecular weight of the polymer [67]

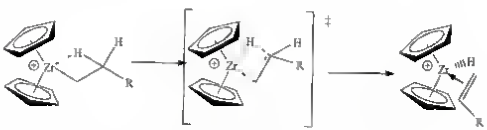

Figure 2-6. β-Hydride elimination reaction[68]

The molecular weight of the polymer depends on the relative rates of the propagation and termination reaction sequences High molecular weight polymers are formed when the rate of propagation is much greater than the termination rate Group four d^0 metals that do not have sufficient electron density to adequately stabilize the β-elimination reaction, exemplify this behavior Conversely when the propagation rate is

slower than the termination rate oligomers and dimers are the dominating products.[68 70] Generally late transition metals that have sufficient electron density to stabilize the olefin complex, via $d\pi$-$d\pi^*$ bonding, produce oligomers and dimers

A key benefit to catalysis that organometallic complexes can offer is that the ligand environment can be easily manipulated to achieve different polymer properties. A good example illustrating the impact a ligand can have on catalyst properties, is the work of Brookhart and co-workers,[71 73] where they were able to produced high molecular weight polyethylene with nickel and palladium catalysts (Figure 2.7) Prior to this work group 10 metal catalysts were found to only oligomerized ethylene.[69 74 75] The crucial feature of these square planar complexes is that the bulky diimine ligands inhibit the associative displacement of the α-olefin (the product of β-elimination) The isopropyl groups of the ligand are situated above and below the square plain of the catalyst that hinders the monomer's access to the metal center Avoiding the displacement by the monomer allows the hydride to re insert into the α-olefin bond resulting in branched high-density polyethylene

There has been an enormous amount of work accomplished in the area of ligand substituents effects and a number of excellent reviews[49,51,53 76] are available describing ligand effects in olefin polymerization processes.

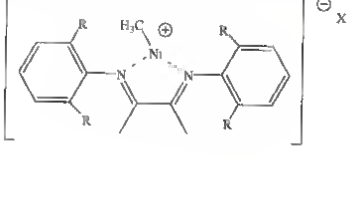

Figure 2-7 Ni(II) diimine catalyst developed by Brookhart produces highly branched HDPE [73]

The particular aspects of the polymerization mechanism that are relevant to this dissertation pertain to the activation of the organometallic precursor. Richardson and coworkers found in earlier work that the interactions between the cationic metal complex and the anion have the highest energy barrier of the polymerization reaction (Figure 2-8).[77-81] Richardson and coworkers illustrated that ion pairing has a significant impact on the polymerization activity. The confirmation was established from the study of the electronic factors that influence the electrophilicity of the metal center and the ion pairing between the metal center and the counterions. Gas phase reactions of group 4 methylmetallocenium ions with various ancillary ligands were studied and found that by increasing the electrophilicity of the metal center increased ion pairing between the metal center and the anion. Increased ion pairing resulted in decreased the polymerization rates due to the occupation of the reactive site by the anion, which does not allow the monomer to coordinate to the metal center. Metal centers that contained ligands with more electron releasing ability were found to have increased polymerization rates due to decreased ion pairing between the metal center and the anion. Therefore controlling the interaction between the anion and the catalyst would be advantageous to overcome the tight ion pairing.

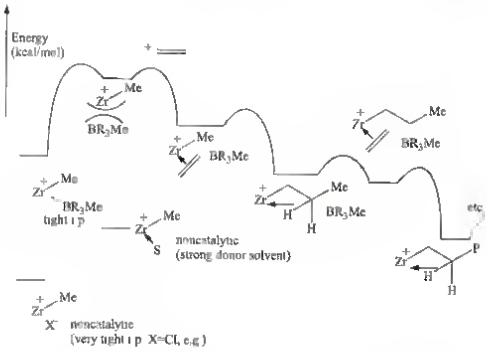

Figure 2-8. Reaction energy diagram for the olefin polymerization mechanism [81]

In 1986 Jordan *et al.* first discovered routes to synthesize and isolate cationic group IV metallocene complexes and showed that it was possible to polymerize ethylene without the use of an aluminium co-catalyst.[82,83] The cationic complex was generated with a one-electron oxidant and trapped with THF (Figure 2-9). The THF ligand is a Lewis base and functions as an inhibitor because it binds tightly to the highly electrophilic metal center. To demonstrate that the complex produced in Figure 2-9 is the active species Jordan and co-workers subjected the complex to an atmosphere of ethylene in CH_2Cl_2 solvent and high-density polyethylene was produced.

Figure 2-9: Generation of a Zirconocene cation[83]

An alternative initiating method developed by Hlatky, Turner, [84] and Bochmann *et al* [85] utilized a tertiary ammonium-tetraphenylborate salt that protonated the metal-alkyl bond of the metallocene generating the active cationic zirconium complex. This method leads to an ionic, basic-free zirconium catalyst which is highly active in toluene. However the reaction is quite complicated; the combination of $(C_5Me_5)_2ZrMe_2$ with $[nBu_3NH][B(p\text{-}C_6H_4Et)_4]$ produces a zwitterionic complex (Figure 2-10), [84] where one of the phenyl rings of the borate anion is metallated. This metallated complex is a result of an electrophilic attack by the intermediate $[(C_5Me_5)_2ZrMe]^+$ cation on the C-H bond of the phenyl ring. The generation of this metallated, zwitterionic species hinders the complexation of the olefin resulting in reduced activity. Although the activity of this system is high, it is still low compared to the MAO-activated system. Further enhancement of the catalytic rate can be accomplished by decreasing the cation-anion interaction by incorporating weakly coordinating anions [86]

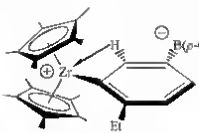

Figure 2-10: Hlatky's Zwitterionic complex[84]

Many weakly coordinating anions (WCA) are based upon perfluorinated arylboranes[87] and borates. Tris-pentafluorophenylborane, first synthesized by Park and

Massey[88,89] is a strong Lewis acid that is capable of abstracting a methyl group from dimethyl zirconocene. Fluorinating the phenyl rings of the borane/borate system has several advantages e.g , enhanced Lewis acidity, increased stability toward protonolysis, improved solubility in non-polar and non coordinating solvents, and increased resistance to electrophilic attack.[87] Tris(pentafluorophenyl)borane combined with (1,2-$(CH_3)_2C_5H_3)ZrMe_2$ abstracts a methyl group producing a highly active catalyst.[90,91] The abstracted methyl group bridges the two highly electrophilic centers (Figure 2-11) resulting in a weakly coordinating cation-anion pair that has activities commensurate to the MAO initiated systems. This pioneering work paved the way for a great deal of research on new larger weakly coordinating anions.

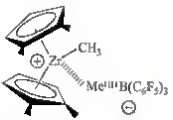

Figure 2-11. Cationic Zirconocene with a μ-methyl-$B(C_6F_5)_3$ bridge.[92-97]

Weakly Coordinating Anions

Over the past few years, the respective groups of Marks and Piers have developed a number of new and effective perfluoroarylborane and bifunctional borane activators. The sterically encumbered perfluoroarylboranes synthesized by the Marks group include tris(2,2',2''-perfluorobiphenyl)borane (PBB),[92] bis(pentafluorophenyl)(2-perfluorobiphenyl)borane (BPB),[94] and tris(β-perfluoronaphthyl)borane (PNB)[93] (Figure 2-12). Activities achieved with these strong Lewis acids have comparable or slightly

higher activities than the $B(C_6F_5)_3$ system. Information obtained from these studies revealed that increasing the steric bulk of the anions does not necessarily afford a more active catalyst. The study revealed that interactions between $Cp_2Zr(CH_3)_2$ and PNB or PBB generated an active species that had activities commensurate with $B(C_6F_5)_3$. The lower than expected rate is a result of competition between the MePNB and the neutral $Cp_2Zr(CH_3)_2$ for the cationic metal complex. Interactions between the $Cp_2ZrCH_3^+$ and $Cp_2Zr(CH_3)_2$ result in a dimeric species $[Cp_2ZrMe(\mu\text{-}Me)MeZrCp_2]^+$ that competes with the olefin and hinders coordination.[93] The formations of dimers vary depending on the coordinating ability of the anion. For example, the anion PBB preferentially forms the dinuclear complex (Zr (μ-Me)-Zr) at room temperature, but increasing reaction temperatures favor the monomeric species. Conversely $B(C_6F_5)_3$ forms the monomeric species exclusively. Further modifications to enhance the Lewis acidity of the fluoroarylborane structure was achieved by Piers[97] and co-workers when they synthesized diboraanthracene (Vb). This diborane compound is a stronger Lewis acid than $B(C_6F_5)_3$ and is somewhat less sterically encumbered than PBB and PNB. The increased Lewis acidity and moderate steric bulk results in a significant increase in polymerization activity up to 20 times the rate of $B(C_6F_5)_3$.[95]

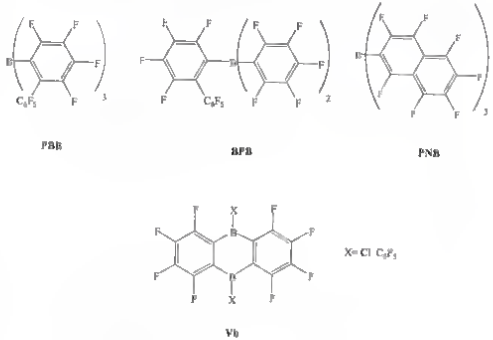

PBB BFB PNB

Vb

Figure 2-12. Weakly coordinating anions [92-97]

Zwitterionic Catalysts

Information obtained during the investigations of WCA systems revealed the large role that the cation-anion interactions have on catalyst activity. Tight ion pairing hinders olefin binding to the metal center reducing the activity of the system. Decreasing the coordinating ability of the anion increases the activity to a point until the separation becomes so large that dimers form. One potential method to gain more control of the cation-anion interaction would be to physically link the borate counterion to the ligand backbone of the catalyst to form a zwitterion. With these zwitterionic species the ion pairing, lifetime of the catalyst, and solubility might be effected

Zwitterionic complexes have been shown to be highly active catalysts. Two different types of zwitterions are described in recent literature. One type of zwitterion has the anion bound directly to the metal center, which through ligand dissociation loses its zwitterionic character. Examples of this type of zwitterion include the ion pair that is created by the combination of Cp_2ZrMe_2 and $B(C_6F_5)_3$ (Figure 2-13 A),[90] Hlatky's complex (Figure 2-13 B)[84] and Erker's π-allyl zwitterion (Figure 2-13-C).[90] Although these complexes are active polymerization catalysts, the borate anion is incorporated into the growing polymer chain, which leads to increased charge separation and potential catalyst deactivation.

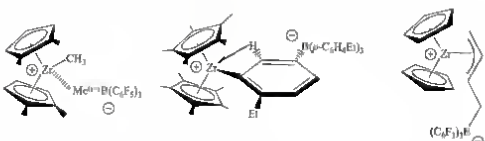

Figure 2-13 Type one zwitterions[84,90-99]

The second type of zwitterion involves complexes that have the borate anion bound directly to the ligand of the catalyst. Our interests focus on this type of zwitterion in order to produce a complex that will preserve the tethered anion during the polymerization process. Examples of this type of zwitterion include Bochmann's complex[100,101] where the $B(C_6F_5)_3$ is directly attached to the Cp ligand (Figure 2-14 A) and Piers's complex[100-103] where borate is tethered to the Cp ring by a methylene linker (Figure 2-14 B). Although these complexes have the anion directly linked to the ligand of the catalyst, the B-C bond is unstable. It has been observed that sp^2 hybridized B-C

bonds are more stable than sp^3 B-C bonds [104] This observation suggests that the more p character that the carbon linker contains the weaker B-C bond will be i.e aryl>cyclopentadienyl>alkyl We recently observed this trend in our laboratory, when the borate moiety attached directly to the cyclopentadienyl ligand ruptured during the metallation of the Cp ligand [105] The presence of boron-carbon bond instability represented in the above examples results in the B-C bond rupture and consequently loss of the zwitterionic nature of the catalyst These observations encouraged us to link the borate moiety to the ligand backbone of the catalyst with a fluorinated phenyl ring. The incorporation of the phenyl linker should sufficiently stabilize the B-C allowing it to remain in tact during the polymerization process.

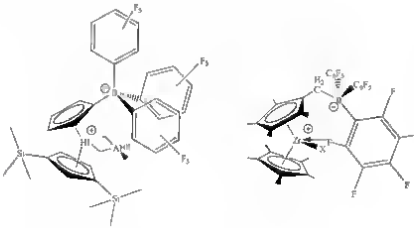

Figure 2-14. Type two zwitterions [100 101 103 106]

Experimental Section

General Considerations All manipulations were performed under an argon atmosphere by using standard Schlenk techniques or under N_2 in a Vac Atmospheres glove box. Glassware was oven dried prior to use Solvents were distilled prior to use

and stored over 4-Å molecular sieves in sealed flasks under argon. Diethyl ether and tetrahydrofuran were dried by distillation from Na/benzophenone ketyl. Pentane was dried by distillation from Na. NMR solvents were purchased from Cambridge Isotopes and were dried over 4-Å molecular sieves and not further purified. TMSCl was purchased from Aldrich and distilled prior to use. Reagents *p*-bromoaniline, *p*-bromo-2,6-dimethylaniline, BPh_3, $Bu_4NF{\cdot}3H_2O$, $ZrCl_4$, LDA (2.0M in heptane/ethylbenzene/THF), and BuLi (2.5M in hexanes) were purchased from Aldrich and used as received. $B(C_6F_5)_3$ was purchased from Boulder Scientific and used as received. The chlorodimethylsilyltetramethylcyclopentadiene was prepared according to a published procedure.[197] ^1H and ^{13}C NMR spectra were obtained by using either a Varian VXR-300 or General Electric QE-300 spectrophotometer. ^{19}F NMR spectra were obtained on a Varian VXR-300. ^{19}F NMR chemical shifts were referenced relative to the fluorine resonance at 0.0 ppm in $CFCl_3$.

$(C_5H(CH_3)_4)$-Si$(CH_3)_2$-*p*-C_6F_4-Br (2-2). n-BuLi (2.90 ml, 2.5M in hexanes) was added slowly to a –78 °C Et_2O solution of 1,4-dibromotetrafluorobenzene (1.43 g, 4.64 mmol) and stirred for 10 min. An Et_2O solution of chlorodimethylsilyl tetramethylcyclopentadiene (1.0 g, 4.64 mmol) was slowly transferred by cannula into the flask containing LiC_6F_4Br over a 10 min period. A light yellow solution formed upon the addition of the second solution. The reaction mixture was stirred for 1 hour at –78 °C, allowed to slowly warm to room temperature and stirred overnight. Solvent was removed to yield a yellow oily solid. The product was then extracted with pentane and cooled to –78 °C yielding a white solid **2-2** (1.40 g, 74%). ^1H NMR (25° $CDCl_3$) δ =

3 21(br s, 1H), 1 79(br s, 12H), 0 21(br s, 6H) ^{19}F NMR (25°, $CDCl_3$) δ = -126 1(m 2F), -133 8(m, 2F) ^{13}C ($CDCl_3$) δ = 10.98, 13 6, 54 0, 110 0, 122.5, 131 9, 136 8, 136 4, 137 0, 140 0, 148 2 Analysis Calc C, 50 27, H 4 43 Found C 50 82 H, 4 84

Li[$(C_5H(CH_3)_4$)-Si(CH_3)$_2$-C_6F_5-*p*-B(C_6F_5)$_3$]·2(*i*-Pr_2O) (2-3). n BuLi (2.75 ml, 2 5M in hexanes) was added slowly to a −78 °C *i*-Pr_2O solution of **2-2** (2 80 g, 6.87 mmol), and the resulting solution was stirred for 10 min. To this solution was added a −78 °C *i*-Pr_2O solution (~100 ml) of B(C_6F_5)$_3$ (3 51 g, 6 87 mmol) The resulting solution turned a slight yellow color Reaction mixture was stirred at −78 °C for four hours allowed to slowly warm to room temperature, and then stirred overnight Upon warming to room temperature a white solid precipitated The solution was then was removed from the white solid by cannula filtration and solid was washed with 10 ml of pentane and dried in *vacuo* yielding **2-3** (5 55g, 77 %) ^{1}H NMR (25°, $CDCl_3$) δ = 0 21 (br s, 6H, -$(CH_3)_2$Si-) 1 15 (d, 24H, *i* Pr_2O), 1 68 (s, 6H, $C_5(CH_3)_4$), 1 71 (s, 6H, $C_5(CH_3)_4$), 3 16 (br s, 1H), 3 90 (mult., 4H, *i*-Pr_2O) ^{19}F NMR (25°, $CDCl_3$) δ = 132 6 (mult., 6F), -133 9 (mult., 2F) -135 4 (br s, 2F), -162.6 (mult 3F) −166 7 (mult 6F)

Li_2[$(C_5(CH_3)_4$)-Si(CH_3)$_2$-C_6F_5-*p*-B(C_6F_5)$_3$]·2(*i*-Pr_2O) (2-4). Compound **2-3** (6 80g, 6 5 mmol) was dissolved in (~ 30 ml) diethylether and stirred for 10 min The diethylether was removed in *vacuo*, and to the resulting solid was added ~ 40 ml of *i* Pr_2O dissolving most of the solid The resulting solution was cooled to −78 °C and added n-BuLi (3 10 ml, 2 5 M in hexanes) to the reaction solution Solution was stirred at −78 °C for two hours, allowed to slowly warm to room temperature and stirred

overnight. As the reaction progressed the solution became clear and then upon warming to room temperature a white precipitate began to appear. Allowed the reaction the stir overnight and removed solvent by cannula filtration and washed white solid with pentane and dried *in vacuo* yielding a white solid **2-4** (6.5g, 95%) ^{1}H NMR (25°, $CDCl_3$) δ = 0.21 (br s, 6H, $-(CH_3)_2Si-$), 1.15 (d, 24H, *i*-Pr_2O), 1.68 (s, 6H, $C_5(CH_3)_4$), 1.71 (s, 6H, $C_5(CH_3)_4$), 3.16 (br s, 1H), 3.90 (mult., 4H, *i*-Pr_2O). ^{19}F NMR (25°, $CDCl_3$) δ = -132.6 (multt., 6F), -133.9 (mult., 2F), -135.4 (br s, 2F), -162.6 (multt 3F), -166.7 (mult. 6F). Analysis Calc. C, 53.31; H, 4.39. Found C, 53.31; H, 4.43.

Li[ZrCl$_2$(C_5H_5)($C_5(CH_3)_4$-Si(CH_3)$_2$-C_6F_4-*p*-B(C_6F_5)$_3$] 2(*i*-Pr_2O) (2-6). A flask was charged with **2-4** (1.01 g) of, 0.25 g of $CpZrCl_3$, and 20 ml of Et_2O was added to the two solids. Immediately both of the solids dissolved and solution turned yellow. Solution was allowed to stir at room temperature and a precipitate started to appear gradually. The reaction mixture was allowed to stir for 5 hours. Solvent was removed *in vacuo* resulting in a yellow oily solid. To this solid was added an additional 20 ml of *i*-Pr_2O to remove the LiCl from reaction mixture. The salts were allowed to settle and removed by cannula filtration. Removal of the solvent from the filtrate under reduced pressure resulted in a yellow-orange solid (.83g, 69%). ^{1}HNMR ($CDCl_3$) δ 0.65 (s, 6H, $-Si(CH_3)_2-$), 1.16 (d, 24 H, iPr_2O), 2.07 (s, 6 H, $C_5(CH_3)_4$), 2.08 (s, 6 H, $C_5(CH_3)_4$), 3.80 (sept. 8H, iPr_2O), 6.30 (s, 5H, C_5H_5). ^{19}F NMR (25°, $CDCl_3$) δ = -132.78 (br d., 2F), -133.3 (mult., 6F), -133.66 (br d, 2F), -162.8 (multt 3F), -166.7 (triplet 2F), -166.96 (mult. 4F). ^{13}C ^{109} (25°, $CDCl_3$) δ =1.813, 12.997, 15.421, 22.679, 70.55, 118.056

130 616, 137 594 Analysis Calc for $C_{52}H_{51}BLi_1O_6Zr$ C, 48 91, H, 4.03 Found C 48 72 H, 4 14

Li[Zr(CH$_3$)$_2$(C$_5$H$_4$)(C$_5$(CH$_3$)$_4$-Si(CH$_3$)$_2$-C$_6$F$_4$-*p*-B(C$_6$F$_5$)$_3$] 3(Et$_2$O) (2-7). A flask was charged with (0 80 g, of **5** and 50 ml of Et_2O resulting in a light yellow solution The solution was cooled to –78 °C and (0 41 ml,) of MeMgBr (3M in Et_2O) was added The resulting solution was stirred at –78 °C for 2 hours and warmed to room temperature Upon warming to room temperature the solution darkened to a light brown color Removal of the solvent *in vacuo* resulted in a light brown oil The oil was extracted with 20 ml of CH_2Cl_2 and filtered The solvent was removed *in vacuo* from the filtrate resulting in a brown crystalline solid ^{1}H NMR (CD_2Cl_2) δ -0 620 (s 6H, Zr(CH$_3$)$_2$) 0 60 (s 6H, Si(CH$_3$)$_2$-), 1 10 (d, 24 H ^{i}Pr$_2$O), 1 81 (s, 6 H, C$_5$(CH$_3$)$_4$), 1 98 (s, 6 H, C$_5$(CH$_3$)$_4$), 3 65 (sept, 8H ^{i}Pr$_2$O), 6 01 (s, 5H, C$_5$H$_5$)

Results and Discussion

Our synthetic scheme for ligand synthesis relies heavily on the kinetic inaccessibility of the methine proton in chlorodimethylsilyl-tetramethylcyclopentadiene(1), as previously exploited by Bercaw et al.[107] Substitution reactions occur at the more kinetically accessible silyl chloride as opposed to deprotonation of the Cp methine proton due to the steric crowding of the tetrasubstituted-Cp ring (Figure 2-15)

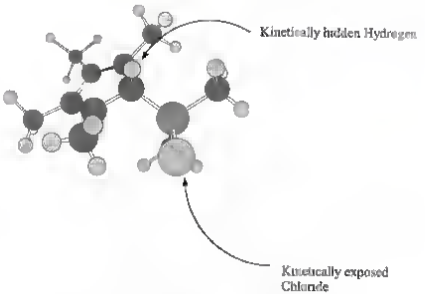

Figure 2-15. Different kinetic reactivity of **2-1**

We took advantage of this relative order of reactivity to attach the tetraphenylborate anion to the Cp ligand. The synthesis of the di-anionic ligand starts with the generation of *p*-bromo-tetrafluorophenyllithium by the addition of *n* BuLi to a THF solution containing 1,4-dibromotetrafluorobenzene. The bromo-lithium exchange reaction produces the highly reactive *p*-bromo-tetrafluorophenyllithium that is trapped by **2-1** to generate compound **2-2** as a light yellow solid in high yield (>80%) after recrystallization from cold hexane (Figure 2-16). The ^{1}H NMR ($CDCl_3$) spectrum of **2-2** exhibits resonances that are readily assigned to the silyl methyl, Cp methyl and Cp methine protons. Only a single resonance is observed for the inequivalent Cp methyl protons. The compound is moderately air sensitive, and decomposes to a deep purple oil upon exposure to the atmosphere.

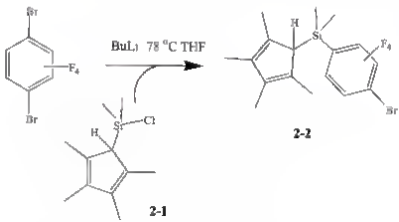

Figure 2-16. Synthesis of **2-2**

The kinetic inaccessibility of the Cp methine proton in **2-2** allows for a second bromine lithium exchange to occur at the more accessible bromine atom of the phenyl ring. We first examined the second halo-lithium exchange reaction in Et_2O solution at –78 °C. However, the reaction does not go to completion and some unidentified products were isolated. Alternative solvents were employed and isopropylether was found to facilitate the formation of compound **2-3** in high yield and purity. Addition of n-BuLi to an i-Pr_2O solution of **2-2** at –78 °C generates the highly reactive *para*-lithium compound rapidly. This product is then trapped by the addition of an i-Pr_2O solution of $B(C_6F_5)_3$ to generate compound **2-3**. Allowing the reaction to slowly warm to room temperature produces the compound (Figure 2-17) as an insoluble white crystalline salt in high yield (>80%).

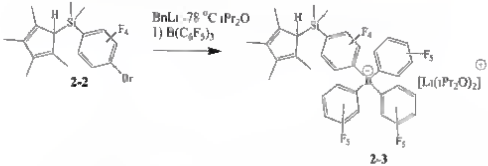

Figure 2-17. Synthesis of Li[$(C_5H(CH_3)_4)$-$Si(CH_3)_2$-C_6F_5-*p*-$B(C_6F_5)_3$] (i-Pr_2O)$_2$ **2-3**

The isolated product turns light purple after sitting in the dry box over a period of a week suggesting thermal instability However, ^{1}H NMR analysis of the light purple compound revealed that very little decomposition had occurred Because **2-3** appears to be unstable over time, it was used as soon as it was produced The difference in reactivity between the different solvents seems to be attributed to the steric bulk of the large isopropyl groups that will only allow two molecules to coordinate to the lithium cation, which in turn facilitates precipitation of the final product The room temperature ^{1}H NMR ($CDCl_3$) spectrum displays resonances at 0.20 ppm corresponding to the $SiMe_2$ group, and 1 70 1 78 ppm for the in equivalent Cp methyl groups In addition the Cp methine proton resonates at 3 18 ppm. Two equivalents of i-Pr_2O were observed by ^{1}H NMR and are presumably coordinated to the lithium counter ion

Removal of the methine proton is necessary in order to generate the desired metal complex. Since compound **2-3** is insoluble in i-Pr_2O, only about 10% conversion was observed when a suspension of **2-3** in i-Pr_2O was treated with n-BnLi This insolubility in i-Pr_2O required us to pursue alternative solvents Reaction was first attempted using Et_2O as a solvent, but little reaction occurred and ligand decomposition was also observed Other solvents employed were CH_2Cl_2, THF, toluene, and benzene,

but to no avail, ligand decomposition was observed in all cases. This reaction is interesting, it appears that the two coordinated isopropylethers on the lithium counterion do not offer sufficient solubility in i-Pr_2O solution for the reaction to proceed. Consequently, changing the coordinated ethers to diethylether, where three molecules will coordinate to the lithium, (by NMR analysis) offers sufficient solubility for the reaction to proceed in isopropylether. Therefore dissolving compound **2-3** in Et_2O, removing the solvent *in vacuo* and replacing the solvent with isopropylether allows the deprotonation to proceed smoothly at –78 °C (Figure 2-18).

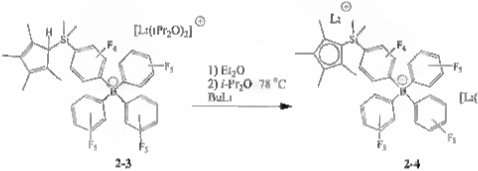

Figure 2-18 Synthesis of $Li_2[(C_5(CH_3)_4)$-$Si(CH_3)_2$-C_6F_5-β-$B(C_6F_5)_3]$ $(i\ Pr_2O)_2$ **2-4**

Initially the reaction solution is cloudy prior to the addition of the n-$BuLi$, but as reaction progresses the solution becomes clear. The reaction mixture is then allowed to warm slowly to room temperature – 4 hours, as reaction solution reaches room temperature compound **2-4** precipitates out of solution as an insoluble white crystalline solid in high yield (>85%). The ^1H NMR of compound **2-4** reveals a new set of resonances that are assigned to an inequivalent set of Cp methyls at 2.0 (6H) and 2.05 (6H) ppm and an equivalent set of silyl methyl protons at 0.625 (6H) ppm.

Attaching the diamonic to the metal center was initially attempted using $ZrCl_4$. Combining the two compounds in Et_2O produced a yellow solution with oil deposited on bottom of flask. Work up of the resulting solution produced a red oily solid that, by ^1H NMR analysis, contained only a small amount of the desired product. Initially the product that formed was yellow, but upon solvent removal, the solid turned red because of decomposition. Given the difficulty associated with the isolation of this complex and that an additional step would be required to complete the formation of the sandwich complex, we decided to use $CpZrCl_3$ as the starting material. An efficient synthesis developed by Livinghouse and others[109] allowed us to produce $CpZrCl_3$(DME) in high yield. Use of this reagent allowed for the sandwich complex to be synthesized in CH_2Cl_2 and isolated as the DME adduct (**2-5**) in good yield. Removal of the DME ligand to produce the base free adduct was attempted by sublimation but was not achieved. Therefore, we purchased the base free $CpZrCl_3$ complex. Generating the sandwich complex was more difficult, low isolated yields resulted from using CH_2Cl_2 as the reaction medium. Using diethyl ether as the solvent allows for the substitution to occur to produce anionic sandwich complex **2-6** (Figure 2-19). The resulting complex is isolated as an air and moisture sensitive yellow-orange powder in good yield (>65%).

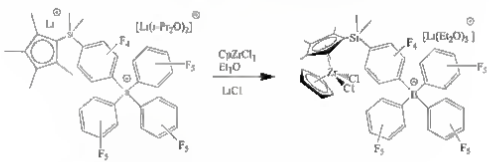

Figure 2-19 Synthesis of the dichloride sandwich complex **2-6**

Our ultimate goal is to form the mono-alkyl zwitterion therefore; according to literature precedent[10] complex **2-6** must be converted to the dimethyl sandwich complex **2-7**. Allowing the dichloride complex **2-6** to react with 2 equivalents of MeMgBr in Et_2O at −78 °C will generate the desired dimethyl complex (Figure 2-20).

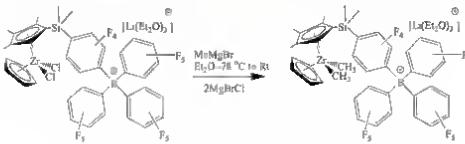

2-6 **2-7**

Figure 2-20. Generation of the dimethyl complex **2-7**

The reaction solution was then concentrated and the resulting solid mixture extracted with CH_2Cl_2. Filtration and solvent removal gave complex **2-7** as a brown solid in greater than 80% yield. The ^1H NMR spectrum of **2-7** displays a resonance at –0.6 ppm that can be attributed to methyl groups that are attached to a high oxidation state metal center. The addition of the alkyl groups shifts the Cp methyl resonances from 2.09 and 2.11 ppm in **2-6** to 1.81 and 1.98 ppm in **2-7**. The Cp protons are shifted up-field from 6.3 to 6.01 ppm. This up-field shift reveals that the metal center has increased electron density at the metal center relative to the dichloride complex, **2-6**.[11]

Isolation of the zwitterion proved to be unattainable with complex **2-7**. Attempts to generate the zwitterion by methyl abstraction led to the formation of a mixture of products. Initial experiments were attempted on small scale by using a couple of different methyl abstracting agents. $B(C_6F_5)_3$ was employed in the presence of acetonitrile which produced a broad peak at 0.5 ppm that is characteristic of

$[H_3CB(C_6F_5)_3]^-$ [112] along with several unidentifiable resonances. The appearance of the methyl borate suggests that this might be possible route to isolate one of the desired product. Therefore, the reaction was attempted on a larger scale using either acetonitrile or toluene as a solvent but isolation of the complex was rather difficult because both reactions produced an only solid that had a very complicated ^1H NMR spectrum.

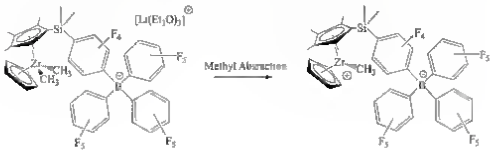

2-7

Figure 2-21–Proposed Zwitterionic complex

An alternative methyl-abstracting agent was employed. The compound $[PhNMe_2H][B(C_6F_5)_4]$ has been shown to be very efficient in generating Zr methyl cations from Cp_2ZrMe_2 derivatives.[113] The reaction was first attempted on small scale in a NMR tube with acetonitrile as a solvent. Immediate methane evolution was observed upon the addition of the ammonium salt to the solution. The ^1H NMR spectrum obtained revealed the loss of the methyl peak at –0.6 ppm and the appearance of two new peaks at –0.03 and –0.2 ppm. Resonances at 1.8 and 2.0 ppm for the Cp methyls in complex **2-7** had changed into 6 peaks after reaction, and the single Cp peak has changed into a doublet. This again seemed to be a feasible route to generating the desired zwitterion complex. Reaction was attempted on a larger scale first with benzene as a solvent but the reaction produced an oil that could not be purified and had a very

complicated ^{1}H NMR spectrum. Since different reactivity has been obtained with different solvents, toluene was employed but was not successful. The spectrum obtained from the oil produced was similar to the benzene reaction, it is important to note the absence of the methyl resonances at ~0.6 ppm but the rest of the spectrum was still very complicated and isolation of the monomethyl zwitterionic species remained elusive. Reasons for the complicated spectra are probably due to the highly reactive species that is generated will react with a number of different species that are present in solution resulting in a complicated mixture of products.

A possible route to isolating the zwitterionic complex would be to trap the product with a lewis base like THF in order to suppress the reactivity of the zwitterion. Therefore a THF solution of **2-7** was subjected to $[PhNMe_2H][B(C_6F_5)_4]$ and the evolution of methane was observed immediately. The ^{1}H NMR confirmed the disappearance of the methyl resonances but the peaks were broad and unresolved. The product of the reaction was a light yellow solid but recrystallization of the isolated solid failed to produce clean product. It appears that the metal center may be too acidic, and experiments should be designed to moderate the Lewis acidity of the metal by incorporating more electron releasing Cp ligands.

X-Ray structural Analysis

Complex **2-6** was heated in isopropylether to 50 °C and allowed cool to room temperature, producing X ray quality single crystals. Selected bond lengths and angles are shown in Table 2-2. The zirconium metal center adopts a distorted tetrahedral configuration with Cl-Zr-Cl and centroid-Zr-centroid angles of 92.28 and 131.3°.

respectively (Figure 2-22). The Zr-Cp* (centroid) and Zr-CpB (centroid) distances are equal at 2.206 and 2.207 Å respectively, as was expected because the electronic make up of the Cp ligands is very similar. It is important to note that the dimethylsilyl linker between the Cp ring and the phenyl ring is situated so that one of the metal chlorides bisects the CH_3-Si-CH_3 angle, allowing the phenyl ring to point away from the metal center. This orientation places the anionic borate ligand as far as possible from the chloride ligands of the zirconium. This orientation minimizes both the steric and electronic repulsions between the anionic borate and the chloride ligands.

Table 2-1. Summary of Crystallographic Data for **2-6**

Empirical formula	C52 H51 B Cl2 F19 Li O2 Si Zr	
Formula weight	1276 89	
Temperature	173(2) K	
Wavelength	0 71073 Å	
Crystal system	Monoclinic	
Space group	P2(1)/c	
Unit cell dimensions	a = 9 7946(4) Å	α= 90°
	b = 34 502(1) Å	β= 102 985(1)°
	c = 16 8584(7) Å	γ = 90°
Volume	5551 4(4) Å^3	
Z	4	
Density (calculated)	1 528 Mg/m^3	
Absorption coefficient	0 419 mm^{-1}	
F(000)	2584	
Crystal size	0 26 x 0 12 x 0 08 mm^3	
Theta range for data collection	1 71 to 27 50°	
Index ranges	-12 ≤h ≤12, -44 ≤k ≤40, -18 ≤l ≤21	
Reflections collected	50496	
Independent reflections	12707 [R(int) = 0 0821]	
Completeness to theta = 27 50°	99 6 %	
Absorption correction	Integration	
Max and min transmission	0 9686 and 0 9055	
Refinement method	Full-matrix least-squares on F^2	
Data / restraints / parameters	12707 / 0 / 727	
Goodness-of-fit on F^2	1 008	
Final R indices [I>2sigma(I)]	R1 = 0 0531, wR2 = 0 1166 [7452]	
R indices (all data)	R1 = 0 1114, wR2 = 0 1430	
Extinction coefficient	0 00040(15)	
Largest diff peak and hole	0 584 and -0 743 e.Å^{-3}	

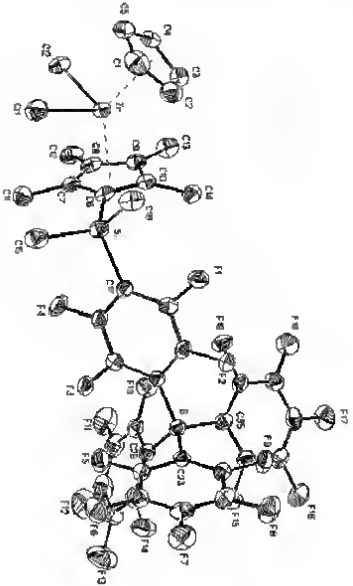

Figure 2-22. Thermal ellipsoid plot for **2-6**

Table 2-2 Selected Bond Distances (Å) and angles (deg) for (2-6)

Zr Cl1	2 4407(11)
Zr-Cl2	2 5033(10)
Zr-centroid (C1-C5)	2 206
Zr-centroid (C6 C10)	2 207
Zr-C6	2 472(3)
Zr-C7	2 525(4)
Zr-C8	2 555(4)
Zr-C9	2 522(4)
Zr-C10	2 522(4)
B-C29	1 642(6)
B-C23	1 644(5)
B-C20	1 648(5)
B-C35	1 667(6)
C18-F1	1 352(4)
Cl1–Zr Cl2	92 28(4)
Centroid Zr-Centroid	131 3
C29-B-C23	113 0(3)
C29-B-C20	113 7(3)
C23-B-C20	102 3(3)
C29-B C35	101 6(3)
C23-B C35	114 1(3)
C20-B C35	112 7(3)
C16-Si-C15	106.3(2)
C16-Si-C6	112 06(18)
C15-Si-C6	114 97(19)
C16-Si-C17	110 45(18)
C15 Si C17	108 07(17)
C6-Si-C17	104 95(16)

Conclusions

The synthesis of a new anionic borate ligand for zwitterionic zirconocene catalysts has been developed The anionic borate ligand is attached to the Cp ring through a robust dimethyl silyl linker that should stay intact during the polymerization process. Metal complexes produced bearing this ligand have been isolated as neutral metallocene complexes Several methods were attempted to generate the mono-methyl

zwitterion, but all routes were unsuccessful The unsuccessful isolation of the zwitterion is probably due the highly reactive metal species that is generated upon the removal of one of the alkyl groups Therefore, to successfully isolate the zwitterion the reactivity of the metal center should be decreased by the incorporation of electron releasing ligands on the metal center

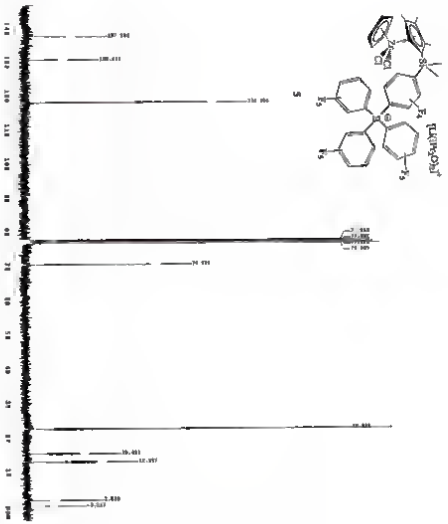

Figure 2-23 ^{13}C spectrum of compound 2-6

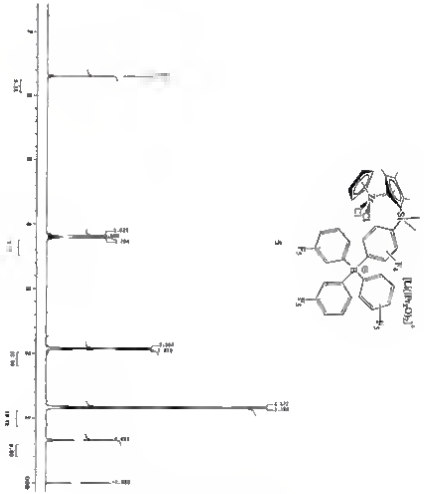

Figure 2-24. H spectrum of compound 2-6.

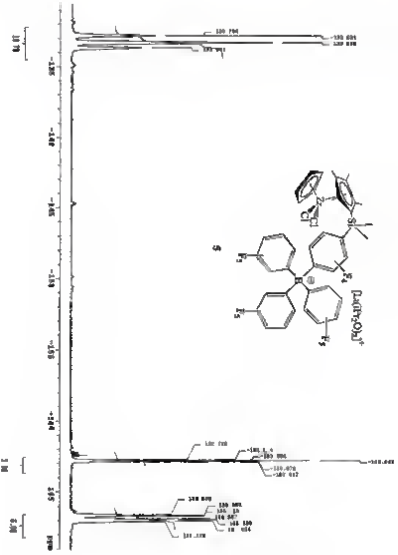

Figure 2-25 ^{19}F spectrum of compound 2-6.

Chapter 3

SYNTHESIS OF BORATE CONTAINING NITROGEN LIGANDS FOR THE USE AS ZWITTERIONIC OLEFIN POLYMERIZATION CATALYSTS

Introduction

As discussed in Chapter 2, there is strong interest in the use of soluble, early and late transition metal catalysts for the polymerization of olefins [114] These well defined systems are highly active and can serve as valuable mechanistic models for the polymerization process Conceivably, the most important aspect of the catalytic systems is the ability to tailor polymer properties by simply altering the catalyst structure and the ligand environment Accordingly, a great deal of research has focused on how ligands affect the catalytic activity and polymer properties [115] Nitrogen containing ligands have had a significant impact on polymerization catalysts, allowing late transition metals (such as Ni, and Pd) to be used as polymerization catalyst,[116-118] and also made the co-polymerization of higher olefins with ethylene more efficient.[119 120]

Bercaw and co-workers[121 122] demonstrated that the reactivity of neutral 14 electron scandocene alkyl complexes could be enhanced by replacing the two cyclopentadienyl rings with a chelating bifunctional *ansa* monocyclopentadienylamido ligand $[(C_5Me_4)SiMe_2(N\text{-}t\text{-}butyl)]^{2-}$ The weaker π-donating character of the ligand enhances the metal's Lewis acidity by reducing the formal electron count of the metal complex by two Steric crowding is also reduced around the d^0 metal center by the replacement of the incredibly bulky pentamethylcyclopentadiene with the amide group

The reduced steric crowding of the metal increases the pocket size of the catalyst and makes an additional vacant molecular orbital available for reaction. Although the rates of ethylene polymerization are relatively slow for these scandium complexes, the ligand system can be applied to other transition metal systems.

Following Bercaw's findings, researchers at Exxon[123] and Dow[124] independently applied the ligand system $[(C_5Me_4)SiR_x(N\text{-}R')]^2$ (R = alkyl, R' = alkyl or aryl) to group 4 metals (Ti, Zr, and Hf) (generally known as constrained geometry catalysts). The constrained geometry catalysts, when in the presence of MAO, are highly active for the co-polymerization of ethylene with α-olefins.[119,125-128] The constrained geometry catalysts allow a ready and random incorporation of the α-monomer over a wide composition range.[129] In general, the open nature of the catalyst does not permit the steric control of α-olefins and generally leads to atactic polymers.[130,131]

Another important class of nitrogen containing ligands are the diimine ligands developed by Brookhart and co-workers.[116-118,132-134] These diimine ligands [ArN=C-(R)-C-(R)=NAr] allowed late transition metals like nickel, (Figure 3.1) and palladium to polymerize ethylene to high molecular weight when in the presence of MAO. In contrast to early transition metal systems, late transition metal catalyst were known to only dimerize or oligomerize olefins due to the facile terminating β-hydrogen elimination reaction.[135] The proposed mechanism of the catalysis is similar to the earlier metal catalysts with the distinct difference that the catalyst can rest as the olefin alkyl complex.[116] Highly branched and amorphous polymers are produced due to the relative stability of the α-olefin resting state. The key function of this ligand is that it retards the associative displacement of the olefin because of the steric bulk of the diimine ligands.

The aryl rings lie roughly perpendicular to the square plane and the ortho substituents block the axial position of the catalyst where associative displacement is known to occur

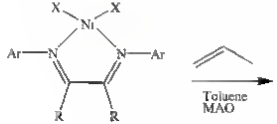

Ar = 2,6-(*i*-Pr)$_2$C$_6$H$_3$ R = CH$_3$ H

Figure 3-1 **Brookhart catalyst**

The distinctiveness of the aforementioned ligands makes them very attractive for use in the preparation of zwitterionic catalysts (figure 3-2) Cation-anion interaction may have a dramatic effect on the activity due to the increased pocket size of the constrained geometry catalyst, and the different pocket shape and size of the diimine catalyst

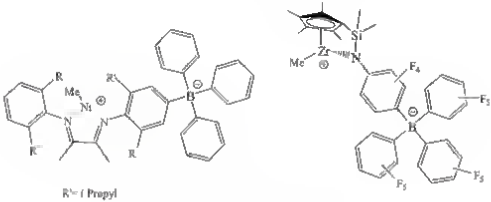

Figure 3-2. Target Zwitterions

Experimental Section

General Considerations

All manipulations were performed under an Argon atmosphere using standard Schlenk techniques or under N_2 in a Vacuum Atmospheres glove box. Glassware was oven dried prior to use. Solvents were distilled and stored over 4-Å molecular sieves in sealed flasks under argon. Diethyl ether and tetrahydrofuran were dried by distillation from Na/benzophenone ketyl. Pentane was dried by distillation from Na. NMR solvents were purchased from Cambridge Isotopes and were dried over 4-Å molecular sieves and not further purified. TMSCl was purchased from Aldrich and distilled prior to use. *P*-bromoaniline, *p*-bromo 2,6 dimethylaniline, BPh_3, $Bu_4NF·3H_2O$, $ZrCl_4$, LDA (2.0M in heptane/ethylbenzene/THF), and BuLi (2.5M in hexanes) were purchased from Aldrich and used as received. $B(C_6F_5)_3$ was purchased from Boulder Scientific and used as received. The chlorodimethylsilyl-tetramethyl-cyclopentadiene was prepared according to a published procedure.[121] Proton and ^{13}C NMR spectra were obtained by using either a Varian VXR-300, Varian Gemini-300, or GE QE 300 spectrophotometer. ^{19}F NMR spectra were obtained on a Varian VXR-300 spectrophotometer. ^{19}F NMR chemical shifts were referenced relative to the fluorine resonance at 0.0 ppm in $CFCl_3$.

***p*-Br-2,6-iPr$_2$C$_6$H$_2$N(TMS)$_2$ (3-1).** To a solution of *p*-Br-2,6-$(CH_3)_2C_6H_2NH_2$ (1.03g, 5.1 mmol) in 40 ml of THF at –78 °C was added LDA (2.57 ml, 5.1 mmol) and solution was stirred for twenty minutes. To this solution was added TMSCl (0.65 ml, 5.1 mmol) and stirred for ten minutes then warmed to room temperature and stirred for an additional thirty minutes. Cooled the resulting light yellow solution to –78 °C was

then added an additional equivalent of LDA (2.57 ml, 5 1 mmol) followed by a second equivalent of TMSCl (0 65 ml, 5 1 mmol). The solution was allowed to warm to room temperature and stirred overnight Solvent was removed *in vacuo* and residue was extracted twice with pentane. The pentane solution was reduced and cooled to –78 °C and filtered and dried, resulting in a light yellow solid yielding **3-1** (1.52g, 86%). ^{1}H NMR (25 °C , C_6D_6)· δ = 7 19(s, 2H), 2.0 (s, 6H), 0 06 (s, 18H)

***p*-Br-2,6-^{i}Pr$_2$C$_6$H$_2$N(TMS)$_2$ (3-2)**. To a solution of [*p*-Br 2,6-^{i}Pr$_2$C$_6$H$_2$NH$_2$]Cl (1 03g, 3 5 mmol) in 30 ml of THF at –78 °C was added LDA (3 5 ml; 7 0 mmol) and solution was stirred for one hour To this solution was added TMSCl (0 45 ml, 3 5 mmol) and allowed solution to warm to room temperature and stirred for one hour. The solution's color lightened as the reaction progressed Resulting solution was again cooled to –78 °C and a second equivalent of LDA (1 75 ml, 3 5 mmol) was added and solution became light yellow, stirred for thirty minutes before a second equivalent of TMSCl (0 45 ml, 3 5 mmol) The solution was allowed to warm to room temperature and stirred overnight Stripped solvent and extracted the residue with pentane 2 x 20 ml The pentane solution was reduced and cooled to –78 °C producing a light yellow solid. Filtered off solid and dried producing **3-2** (1 33 g, 94%) ^{1}H NMR (25 °C , C_6D_6) δ – 7 31(s, 2H), 3 40 (sept, 2H) 1 04 (d, 12H), 0 06 (s, 18H)

Li[*p*-BPh$_3$-2,6-(CH$_2$)$_2$C$_6$H$_2$N(TMS)$_2$] (THF)$_4$ (3-3) To a solution of **3-1** (1.6 g, 4 6 mmol) in 50 ml of THF at –78 °C was added BuLi (1 86 ml, 4 6 mmol) and solution was stirred for 30 minutes To this solution was added a –78 °C THF solution (~20 ml)

of $B(C_6H_5)_3$ (1 11 g, 4 6 mmol) The resulting light yellow solution was stirred at –78 °C for an hour and then allowed to warm slowly to room temperature and stirred overnight The solvent was removed *in vacuo*, resulting in a yellow oil Tha oil was washed 3 x 20 ml of pentane yielding a white solid Solid was dried *in vacuo* yielding **3-3** (2 8 g, 75%). ^1H NMR (25 °C, C_6D_6) δ = 7.58 (br d, 6H), 7.19 (br s, 2H) 7 02 (t, 6H), 6 85 (t 3H) 3 50(sept, 8H), 2 15 (s, 6H), 1 5 (mult 8H), 0 05 (s, 18H)

Li[*p*-BPh$_3$-2,6-*i*Pr$_2$C$_6$H$_2$N(TMS)$_2$] (THF)$_4$ (3-4) To a solution of **3-2** (1 45 g, 3 6 mmol) in 50 ml of THF at –78 °C was added BuLi (1 44 ml, 3 6 mmol) and solution was stirred for 30 minutes. To this solution was added BPh_3 (87 g, 3 6 mmol in 20 ml of THF) The resulting yellow solution was stirred at 78 °C for an hour and then allowed to warm slowly to room temperature and stirred overnight. The solvent was stripped yielding a yellow oil, which was washed 3 x 20 ml of pentane resulting in a white solid **3-4** (2.0 g, 65 %) ^1H NMR (25 °C , C_6D_6) δ ~ 7 92 (br d, 6H), 7 5 (br s, 2H), 7 21 (t, 6H), 7 01 (t, 3H), 3 61(sept, 2H) 3 1 (m, 16H), 1.39 (d, 12H) 1.2 (m, 16H) 0 2 (s, 18H)

NBu$_4$[*p*-BPh$_3$-2,6-(CH$_3$)$_2$C$_6$H$_2$NH$_2$] (3-5) A schlenk flask was charged with **3-3** (1 0 g 1 25 mmol) and TBAF (1 57 g 4 99 mmol) 30 ml of THF was added to the mixture resulting in a light brown solution The resulting solution was heated to 70 °C and stirred for two days Over the period of the reaction the solution turned dark brown The resulting dark brown solution was stripped of the solvent yielding a brown oil The oil was washed two times with ~ 20 ml of H_2O producing a tan solid. The tan solid was

collected by filtration and let air dry yielding **3-5** (0 75 g, 91%) ^{1}H NMR (25 °C, CD_3CN/C_6D_5). δ = 7 61 (br s., 6H), 7 1 (br s., 2H), 7.0 (t, 6H), 6.82 (t, 3H), 3 20 (s, 8H), 3 10 (br s 2H), 2 5 (mult 8H), 1 98 (s, 6H), 1 20 (mult 8H), 0 85 (t, 12H)

NBu$_4$[*p*-BPh$_3$-2,6-(*i* Pr)$_2$C$_6$H$_2$NH$_2$] (3-6) A schlenk flask was charged with **3-4** (1 0 g, 1.12 mmol) and TBAF (1 9 g, 5 4 mmol) and the solids were dissolved with ~ 30 ml of THF The yellow solution was heated to 70 °C and stirred for four days The resulting dark brown solution was stripped of the solvent yielding a brown oil Washed the resulting oil was washed with ~ 20 ml of H_2O which resulted in a tan solid The tan solid was collected by filtration and let air dry yielding **3-6** (0 78 g, 94%) ^{1}H NMR (25 °C, CD_3CN/C_6D_6) δ = 7 40 (mult., 8H), 7 0 (t, 6H), 6.8 (t, 3H), 3 42 (br s, 2H), 3 10 (mult 8H) 2 9 (sept. 2H), 1.6 (mult 8H), 1 35 (mult 8H), 1 16 (d 12H), 1 0 (mult., 12H)

***p*-Br-C$_6$F$_4$N(TMS)$_2$ (3-7).** To a solution of *p*-Br-C$_6$F$_4$NH$_2$ (1 69g, 6 93 mmol) in 30 ml of THF at –78 °C was added LDA (3 45 ml, 6 93 mmol) and allowed to stir for thirty minutes To the resulting solution was added TMSCl (0 88 ml, 6 93 mmol), the solution turned colorless immediately Allowed the solution to warm to room temperature and stirred for an additional hour Resulting solution was again cooled to 78 °C and a second equivalent of LDA (3 45 ml, 6 93 mmol) was added and allowed to stir for thirty minutes before a second equivalent of TMSCl (0 88 ml, 6 93 mmol) was added The resulting reaction solution was allowed to warm to room temperature and stirred overnight Stripped off solvent and extracted the residue with pentane 2 x 20 ml

Reduced the extract and cooled to –78 °C producing a light brown solid. Removed the remaining solvent and pumped the solid to dryness. Allowing the solid to warm to room temperature results in the solid melting producing a viscous brown oil. **3-7** (2.02 g, 75%) ^{1}H NMR (25 °C , C_6D_6) δ = 0.06 (s, 18H), ^{19}F NMR (25 °C , C_6D_6) δ = –135.43 (d, 2F) -145.25 (d, 2F)

Li[*p*-B(C_6F_5)$_3$-C_6F_4N(TMS)$_2$] (*i*-Pr_2O)$_2$ (3-8). To a solution of **3-7** (1.15 g, 2.96 mmol) in 20 ml of *i*-Pr_2O at –78 °C was added *n*-BuLi (1.18 ml, 2.96 mmol) and allowed to stir for thirty minutes until a white precipitate appeared. B(C_6F_5)$_3$ (1.51 g, 2.96 mmol) was dissolved in 20 ml of *i*-Pr_2O and added to the reaction mixture. The reaction was allowed to stir for at –78 °C for three hours then warmed to room temperature. Upon warming a white precipitate began to come out of solution. Allowed the solution stir for an additional three hours, then solution was decanted form the white precipitate. The resulting solid was washed with an additional 10 ml of *i*-Pr_2O and pumped to dryness producing **3-8** (2.60 g, 85%) ^{1}H NMR (25 °C , C_6D_6). δ = 3.23 (sept, 4H), 0.80 (d, 24H), 0.101 (s, 9H) -0.019 (s, 9H), ^{19}F NMR (25 °C , C_6D_6) δ = -133.92 (br s, 4F) -134.57 (br s, 2F), -138.24 (br s, 2F), -154.21 (br s, 2F), -162.9 (br s, 3F), -167.41 (mult, 4F), -167.91 (br s, 2F)

NBo$_4$[*p*-B(C_6F_5)$_3$-$C_6F_4NH_2$] (3-9). A flask was charged with **3-8** (1.78 g, 1.72 mmol) and TBAF (2.42 g, 6.88 mmol). To the solid mixture was added 30 ml of THF and solution was heated to 70 °C and stirred for 36 hours. As reaction progressed the solution turned a dark brown. Cooled the reaction solution to room temperature and

reduced solution by 75% 20 ml of H_2O was added to the reduced solution producing a white precipitate Filtered the white precipitate and washed with an additional 20 ml of H_2O dried in air producing **3-9** (1 30 g, 85 %) ^1H NMR (25 °C , C_6D_6/CD_3CN) δ = 3 23 (br s, 2H) 2 50 (mult. 8H) 1 75 (s, 8H) 1 1 (mult , 8H) 0 80 (mult , 12H), ^{19}F NMR (25 °C , C_6D_6) δ = -131 5 (mult., 6F), -134 2 (mult., 2F), -162 5 (t, 2F), -162 9 (t, 1F), -163 4 (dd, 2F), -166.3 (mult , 6F)

PPN[*p*-B(C_6F_5)$_3$-$C_6F_4NH_2$] (3-10) A flask was charged with **3-9** (0 75 g, 0 84 mmol) and PPNCl (1 00 g, 1 74 mmol) then dissolved in 25 ml CH_3CN The resulting solution was stirred for three hours and then reduced the solvent by 50 %. 20 ml of H_2O was then added to the solution yielding a white precipitate The white solid was allowed to dry in air yielding **3-10** (0 70 g, 74 %) ^1H NMR (25 °C , CD_3CN) δ = 7 60 (mult , 30H), 4 15 (br s, 2H), ^{19}F NMR (25 °C , CD_3CN) δ = -132.42 (mult., 6F), -135 32 (br s, 2F), -163 14 (t, 2F), -163 33 (t, 1F), -164 5 (dd, 2F), -167.38 (mult., 6F)

PPN[*p*-B(C_6F_5)$_2$-C_6F_4NH[$SiMe_2$(HC_5Me_4)] (3-11). To a solution of **3-10** (0.30 g, 0 27 mmol) in 20 ml of THF at -78 °C was added *n*-BuLi (0.10 ml, 0.27 mmol) and allowed to stir for two hours Allowed the solution to warm to room temperature and removed solvent *in vacuo* resulting in oil Product was extracted with 10 ml of THF and product was precipitated with 10 ml of pentane. A yellow solid was collected by filtration and dried *in vacuo* yielding **3-11** as a light yellow solid (0 17 g, 50 %) ^1H NMR (25 °C , CD_3CN) δ = 7 50 (mult , 30H), 4 15 (br s, 1H), 3 05 (br s, 1H) 1 83 (s,

6H), 1 72 (s, 6H), 0 12 (s, 6H), ^{19}F NMR (25 °C , CD_3CN) δ =–132 42 (mult., 6F), –135 0 (br s, 2F), -160 0 (mult., 2F), -163 14 (t, 2F), -163 33 (t, 1F), -167 3E (mult , 6F)

Results and Discussion

Our research interest has focused oo preparing transition metal complexes that contain a nitrogen ligand with a covalently linked borate anion One approach to obtaining this goal is an aniline-based synthesis developed in our group by Miller[136] This synthesis method can be applied to two different ligand systems. The diimine ligand originally used by Brookhart and co-workers[116-118,132-134] for the polymerzatioo of olefins with late transition metals like iron, nickel, and palladium The second type is the constrained geometry ligand first developed by Bercaw and co-workers[121-122] that can be applied to group four metals These relatively new ligands offer a very good opportunity to attempt the preparation of zwitterionic complexes

The diimine ligands used for late transition metal consists of two components a substituted anilhae and di-ketone Therefore we chose to prepare borate-containing anilines that we could then condense onto the di-ketone to prepare the anionic diimine ligand The synthesis is accomplished by first protecting the amine group of the aniline with trimethylsilane (TMS) groups TMS was the protecting group of choice because of their stability toward strong bases and they can also be easily removed without employing strong acids, to which the borates are sensitive[137]

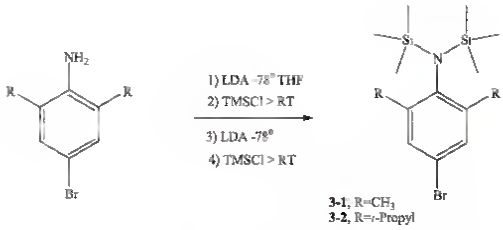

Figure 3-3 Synthesis of the protected aniline

Protection of the anilines is easily accomplished (Figure 3-3) in THF by the stepwise addition of one equivalent of lithium diisopropylamide (LDA) followed by the addition of trimethylsilylchloride (TMSCl). This procedure is then repeated to produce the fully protected aniline. It is possible to add 2 equivalents of LDA, followed by the addition of 2 equivalents of TMSCl, but cleaner products are obtained from stepwise addition. Extracting **3-2** with hexanes to separate from the LiCl, and cooling the resulting hexane solution to -78° C yields a light yellow crystalline solid in high yield (>80%). Isolation of **3-1** was similar to the above reaction with the exception that it was isolated as a light brown solid also in high yield (>75%)

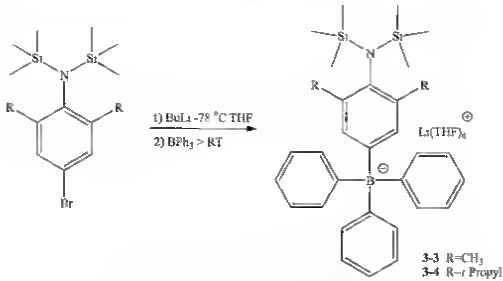

Figure 3-4. Synthesis of the *p*-borateaniline

Attaching the borane to the protected anilines can be achieved by the addition of a THF solution of n BuLi at -78 °C followed by the addition of a THF solution of triphenylborane (Figure 3-4) The bromo-lithium exchange reaction is complete within 30 minutes the subsequent addition of the BPh_3 yields the lithium salt of the *para*-boratoanilines Yields of these reactions are good >80% and can be achieved on a multi gram scale

Deprotection of these compounds has proved rather difficult There are several methods that can be applied to this system for the removal of the TMS groups from the aniline [138] Methanolysis was first attempted but decomposition of the borate moiety was observed The methanol mixture showed no reactivity at room temperature, but heating the methanolic solution to 50 °C or higher did result in removal of the TMS groups but borate decomposition was observed

An alternative method, for the removal of the silyl groups reported in the literature indicates that the fluoride ion is an effective desilylation agent.[139-141] The nucleophilic fluoride ion can attack the silicon atom of compound **3-3, 3-4** to generate trimethylsilylflouride (TMSF) and an anilide anion. The anilide anion is then protonated by the solvent or trace amounts of water present in solution. Generation of the strong Si–F bond and the formation of volatile TMSF by-product is the driving force for this reaction. Generally, there are two sources of the fluoride ion, alkali metal fluorides and tetra-alkylammonium fluorides. The literature suggests that the best source of the fluoride ion is an acetonitrile solution containing KF with 18-crown-6 [142] 18-crown-6 is employed to enhance the solubility of KF in the aprotic media. The KF/ 18-crown 6/CH_3CN mixture reacted very slowly with the protected anilines, reaction was allowed to stir at 80 °C for five days and only ca. 30% of the deprotected product was observed, by ^1H NMR. The high concentrations of the reactants employed and long reaction times made isolation of the products very difficult, therefore this system showed little promise for the deprotection of the aniline borates.

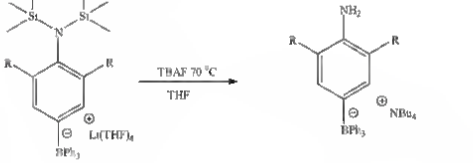

3-5 R=CH_3
3-6 R=i Propyl

Figure 3-5. Deprotection of the aniline borate

An alternative fluoride source is the readily available tetrabutylammonium-fluoride tri-hydrate (TBAF). TBAF has some advantages over the alkali metal fluoride system, it is soluble in THF, and the reaction can be performed at low temperatures. A disadvantage associated with this reagent is that it is very hydroscopic and the water cannot be removed without decomposing the compound. Borates are not sensitive to trace amounts of water therefore this reagent could be applied to this system to remove the TMS protecting groups. Reacting excess amounts of TBAF in THF at 70 °C (Figure 3-5) produces compounds **3-5** and **3-6**. Depending on the ortho substituents of the aniline, the reaction can be complete within 2-5 days. The mechanism[143] is believed to be the same for both systems (Figure 3-6) where the fluoride anion attacks the Si of the protected aniline to produce an anilide intermediate, which then reacts with one of the water groups of the TBAF forming a NH bond. The process is then repeated to produce the fully deprotected product. Although the reaction consumes only two equivalents of TBAF, the reaction requires an excess amount of TBAF to drive the reaction to completion.

The reaction is dependant on the amount of TBAF used, using just two equivalents reaction did not go to completion. Conversely using ten-fold excess the reaction is complete in 24 hours, but isolated products were oily and proved to be difficult to purify. Optimum conditions consist of four equivalents of TBAF in THF at 70 °C. Products are isolated as an oil, then washed with water producing a light brown solid. The lithium cation gets displaced in the THF solution by the NBu^+ cation.

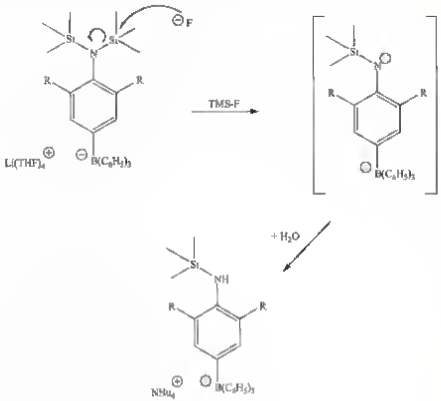

Figure 3-6. Mechanism of deprotection of the aniline borate

The difference in reactivity between the KF system and the TBAF system can be attributed to the difference in ion pairing between the two cations. KF is not very soluble in solution even with the crown ether present, therefore reducing the amount of fluoride ion in solution. Ion pairing between the large tetrabutylammonium cation and the fluoride anion is minimal in THF solvent. In solution this F^- ion can be described as "naked" meaning that the ion acts independently. Reduced interaction between the cation and anion increases the nucleophilicity of the fluoride ion. This increased nucleophilicity promotes attack at the silicon to generate the amide intermediate.

Protonation of the intermediate by H_2O and repeating attack at the silicon generates the desired products **(3-5, 3-6)**

Once the deprotected anilines is obtained the next stage is to prepare the diimine ligand. Imines are best prepared by an acid catalyzed reaction in the presence of a ketone (Figure 3-7)[144]

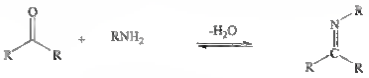

Figure 3-7 Schiff Base Reaction

In general, for Schiff base reactions ketones react slowly and often require high temperatures and extended reaction times along with the use of an acid catalyst. Most often the equilibrium must be shifted, usually by removal of water from the reaction using dehydrating agents such as molecular sieves or $MgSO_4$ or by the removal of the imine through precipitation. The reaction of 2,6 diisopropylaniline with 2,3-butanedione cleanly affords the symmetric diimine ligand. This reaction in the presence of formic acid, proceeds smoothly in methanol at room temperature to give the diimine as a yellow solid

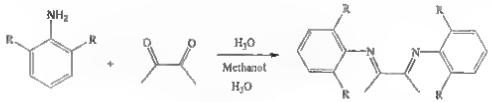

Figure 3-8. Preparation of a diimine

This reaction cannot be applied to the borate containing anilines due to the acid sensitivity of the borate moiety. Since the imine forming reaction is in equilibrium,

methods applied for the synthesis of the asymmetric p-borate containing diimine concentrated on shifting the equilibrium to the product side [145] Molecular sievas were first employed as a dehydrating agent to remove the water produced during the reaction that would drive the equilibrium to the desired product The reaction was stirred at reflux for three days, after work up only the starting materials were recovered $MgSO_4$ was also used as a dehydrating agent under the same conditions as the molecular sieve reaction, and the same result was obtained Literature has suggested that a 3 1 mixture of CH_2Cl_2/MeOH will condense a primary amine onto a ketone without the aid of a catalyst [146] This co-solvent reaction mixture was stirred at reflux for four days and no apparent reaction had occurred These methods have offered very little success to produce the p-borate substituted diimines, therefore other methods should be sought to provide the most convenient and practical method to produce the asymmetric diimine ligand

Constrained geometry

The synthesis of the borate containing amines can also be applied to the constrained geometry ligand system For this ligand system we chose to employ the fluorinated aniline and fluorinate borane for the same reasons that were introduced in chapter 2 The synthesis of the borate-amine is similar to that of the methyl and isopropyl substituted anilines **3-5** and **3-6** Protecting the fluorinating aniline produces compound **3-7** as brown oil at room temperature in high yield (>75%) ^1H NMR spectrum for **3-7** displays a single peak at –0 007 ppm while the ^{19}F NMR displays two sets of doublets at –135 43 and 145 26 ppm Cooling the isolated oil to 4 °C solidifies the compound, which makes for easier handling Attaching the

tris(pentafluorophenyl)borane to the aniline is accomplished in the presence of BuLi in *i* Pr_2O solution at −78 °C. The solution was allowed to stir at −78 °C for three hours and allowed to warm to room temperature slowly producing compound **3-8** as a white crystalline solid in high yield (>85%). The ^1H NMR (C_6D_6) spectrum changes significantly the TMS groups split into two singlets at −0.019 and 0.101 ppm; these peaks are accompanied with the *i*-Pr_2O resonances. The ^{19}F also changes significantly; resonances associated with the anilino have broadened and shifted up field to −132 and 154.2 ppm, resonances associated with the borate anion appear at −134, −162.9, and −167.5 ppm.

Deprotection of **3-8** can be accomplished in the same manner as with the previous anionic compounds, with TBAF. The reaction proceeds smoothly in THF, requiring only 24 hours for the reaction to be completed. Compound **3-9** is isolated, after washing the brown oil with water, as a white crystalline solid in good yield (>70%) with NBu_4^+ as the counterion. The ^1H NMR is remarkably clean containing only three resonances associated with the NBu_4^+ cation at 0.80, 1.15, and 2.45 ppm. While the amine protons resonate with a broad singlet at 3.42 ppm. The ^{19}F NMR reveals that the aniline fluorines have shifted significantly, *ortho* fluorines resonate at −163 and *meta* fluorines resonate at −134 ppm.

Procedures for the construction of the constrained geometry ligand consists of the deprotonation of the aniline and then reacting with $(C_5Me_4)SiMe_2Cl$. The tetrabutylammonium cation however is reactive towards BuLi that subsequently generates NBu_3 and butene as by-products. Exchanging the cation with the non-reactive Bis(triphenyl-phosphoranylidene)ammonium chloride (PPN) will produce compound **3-**

10, which allows for the deprotonation with BuLi to occur. The deprotonated aniline is generated in THF and then trapped by $Me_4C_5HSiMe_2Cl$ to produce the monocyclopentadienylamido ligand compound **3-11** (Figure 3-9). The ligand is isolated as a light yellow solid in relatively low yield (<65%).

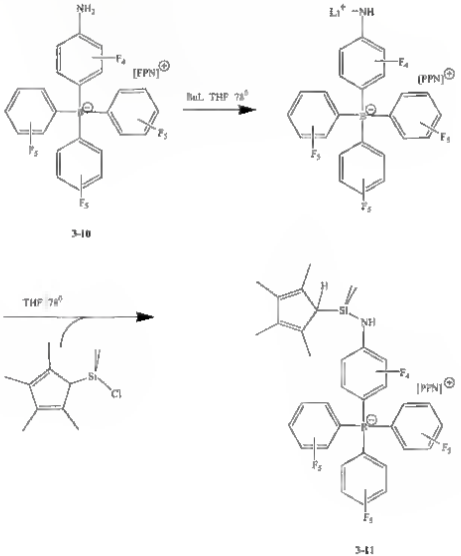

Figure 3-9 Constrained geometry ligand synthesis

Two procedures are available to complex this anionic ligand to an electrophilic group four metal center. Bercaw's[122,147] approach utilizes the methanis reaction of the dilithio salt of $[CpL(NR^-)]^2$ with the metal halide. Okuda and co-workers[148,149] have employed this strategy to synthesize a variety of Zr and Ti compounds. Unfortunately this route leads to low isolated yields and produces a mixture of products.

An alternative strategy employs the amine elimination reaction[150] recently employed by Teuben and co-workers[120,125] for the synthesis of ansa monocyclopentadienyl amido complexes with a two or three alkyl chain linker. This method was employed by reacting compound **3-11** with $Zr(NMe_2)_4$ in toluene at 50 °C under argon flow. The reaction showed several reaction products, one of which appeared to be the metallated product **3-12**, but separation of the reaction mixture was attempted but was not successful due to the same solubility properties of all the products. Alternative solvents were employed to attempt to change the product distribution but these attempts were also unsuccessful.

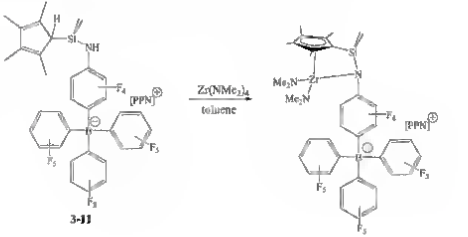

Figure 3-10 Metallation of compound **3-11**

Chapter 4

OXIDATION OF CYCLOHEXANE WITH FE(II) CATALYSTS

Historical Development

Oxidation of organic compounds has been of interest to humanity since the discovery of fire. Some of the basic understanding of oxidation came from Lavoisier and his explanation of combustion, which marked the modern era of oxidation chemistry.[151] Initial studies of oxidation came during the early nineteenth century that related the deterioration of organic materials, like rubber and natural oils, to the absorption oxygen. The initial investigations on oxidation reactions were focused on the inhibition of the oxidative degradation process. Modern mechanistic understanding of the oxidation process was not developed until the 1940 s when the theory of autoxidation was presented to describe free-radical chain chemistry.[151] Autoxidation can be defined as an oxidation reaction of an organic substrate with molecular oxygen, usually occurring via a free radical chain process. Since the 1940's, a vast body of literature has accumulated on hydrocarbon oxidation. These studies agree on the basic underlying principles of oxidation, but several important points remain in disagreement due to the complex nature of even the simplest materials. The scope of oxidation chemistry is massive and incorporates a wide range of reactions and processes. This dissertation chapter will provide a brief introduction to the homogeneous catalytic oxidations of hydrocarbons.

Autoxidation processes consist of a very large number of radical reactions that occur simultaneously [152] These reactions can be spontaneously initiated, but are usually promoted by trace quantities of metal complexes Although autoxidations are generally highly exothermic reactions, they do not readily undergo spontaneous combustion in air, largely owing to the high activation energies for initiation. In other words, aerial oxidations are difficult to initiate, but once the reaction is initiated, it is often difficult stop short of the fully oxidized products, namely carbon dioxide and water Control of these autoxidation reactions is essential, from an industrial standpoint for promoting selective oxidation of organic feedstocks to produce a variety of useful chemical reagents

Soluble transition metal complexes play an important role in selective oxidation of hydrocarbon substrates Metal catalyzed hydrocarbon oxidations represents one of the most challenging and important transformations in the chemical industry [151,153,154] Metal-catalyzed liquid phase oxidations are used for many large-scale oxidation processes Some early applications of homogeneous liquid-phase catalytic oxidations came in the late 1950's when the Mid Century and the Wacker processes were introduced to industry

The Wacker process involves a palladium-catalyzed oxidation of ethylene to acetaldehyde in water (figure 4-1) Mechanistically this process incorporates two catalytic cycles

Figure 4-1, Wacker process, conversion of ethylene to acetaldehyde

oxidation of ethylene by Pd^{2+} and water (which leads to elimination of acetaldehyde and reduction of Pd^{+2} to Pd^{0}), regeneration of the catalyst Pd^{2+} by the oxidation of Pd^{0} by Cu^{2+} (Cu^{+2} is reduced to Cu^{+1}). Finally the Cu^{2+} catalyst is regenerated by air oxidation (Figure 4-2) [151] This homogeneous catalytic oxidation is carried out at 100-110 °C and 150 psi of ethylene and air producing acetaldehyde in high yield (>95%). The drawback to the Wacker system is that the reaction solution is highly corrosive due to the presence of Cl ions and oxygen in the system. The corrosive nature of the system requires the use of special alloy materials that adds to the cost of production of acetaldehyde. Nonetheless the relative mild reaction conditions (100 – 110 °C) and the high efficiency (>90 %) of the Wacker process make it a viable industrial process for the production of acetaldehyde.

The Mid-century process involves the oxidation an olefin to an epoxide. Selective oxygen atom transfer from the metal catalyst to the olefinic substrate is the principle product forming reaction [156-160] The source of oxygen in these systems is usually an organic peroxide rather than molecular oxygen. Complexes of metals in low oxidation states, like $Mo(CO)_6$, and $W(CO)_6$, can be rapidly oxidized to their high oxidation states by the presence of organic peroxides. The mechanism has two competing transformations associated with this reaction, molybdenum-catalyzed peroxide decomposition, initiated by electron transfer between Mo(V) and Mo(VI), and the molybdenum-catalyzed epoxidation by Mn(VI). The Mo(VI)-hydroperoxide complex has been determined to be the active species for the epoxidation of olefins (Figure 4-3). [159] T-butyl peroxide is consumed in the reaction, which adds to the cost of

the production of epoxides. This process is still an efficient process for the production of epoxides is still in use today

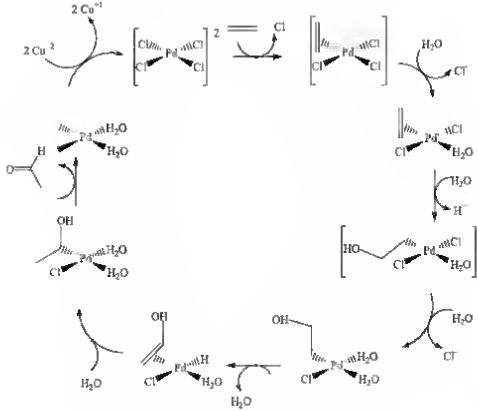

Figure 4-2. Catalytic cycle for Wacker oxidation of ethylene to acetaldehyde.[155]

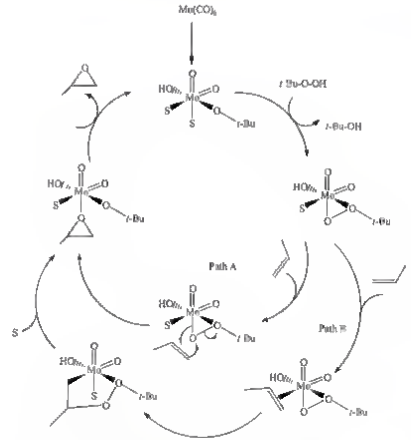

Figure 4-3 Mo(VI) catalyzed epoxidation of propylene in the presence of *t*-butyl peroxide. Paths A and B are two different proposed pathways, in which neither can be ruled out [29]

Another more recent example of homogeneous oxidation involves the oxidation of cyclohexane by molecular oxygen. This type of reaction can be classified as an autoxidation reaction. As mentioned earlier, autoxidation reactions can occur without the presence of a catalyst but the reaction can be enhanced with the use of soluble transition metal catalysts. Cobalt and manganese carboxylate salts have been used to initiate the free radical reaction by acting as a peroxide decomposition catalyst. The role of the catalysts is considered to be a peroxide decomposition catalyst. Metal catalysts

can interact with the peroxide in a couple of different ways (equation 1and 2) The decomposition products can then propagate the radical chain reaction

$$ROOH + M^{+2} \longrightarrow RO^{\cdot} + HO^{-} + M^{+3} \quad (1)$$

$$ROOH + M^{+3} \longrightarrow ROO^{\cdot} + H^{+} + M^{+2} \quad (2)$$

Cyclohexane oxidation is of considerable importance because it is the common starting material in the production of adipic acid, one of the main ingredients in nylon 6 6. The polyamide nyloo 6 6 is among the largest volume synthetic chemicals produced in the world each year with a current global production of ca. 2 million metric tons [161] This oxidation reaction proceeds in two steps, the first of which involves the oxidation of cyclohexane by oxygen in the presence of Co / Mn catalyst to produce cyclohexanol and cyclohexanone Cyclohexanol and cyclohexanone are then further oxidized by nitric acid in the presence of V^{+5} and Cu^{+2} ions to selectively produce adipic acid [162] This process (equation 3) is very efficient and produces high purity adipic acid

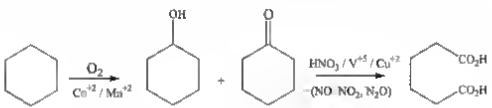

(3)

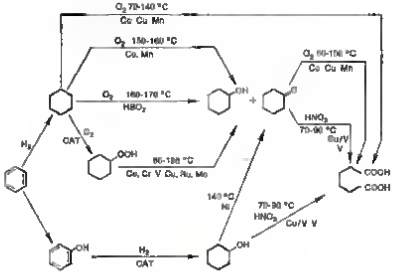

Figure 4-4 Industrial routes for the production of adipic acid [163]

The oxidation of cyclohexanol and cyclohexanone by nitric acid is the most efficient way to produce high purity adipic acid. Nitric acid is consumed by the reaction (equation 3), which in turn leads to the generation of large amounts of NO_x and N_2O gases produced. The nitrogen containing gases released from the reaction have been implicated in global warming [164] Due to the increasing environmental restrictions of introducing greenhouse gasses into the environment alternative routes have been sought for the complete transformation of cyclohexane to adipic acid.

The pursuit of this goal has developed quite diverse heterogeneous and homogeneous systems [165] Thomas and coworkers developed iron and cobalt containing molecular sieves that have been shown to oxidize cyclohexane[166] and n hexane[167 168] to

adipic acid The pore size of the solid acid catalysts is said to control the reactivity and selectivity of the oxidation Iron and cobalt containing molecular sieves that have pore sizes commensurate with that of the cyclohexane molecule have been shown to oxidize cyclohexane to adipic acid, with conversions to adipic acid about 3-4% and long reaction times 15 20 hrs.[166]

Interesting examples of homogeneous systems include the work of Tanaka and co-workers[170] where a relatively high concentration (0 01-0 04 M) of cobalt(III) acetate was employed in an acetic acid medium

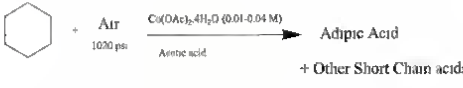

Figure 4-5 Oxidation of cyclohexane in acidic acid[170]

Tanaka's system can reach up to 80% conversion and 70% selectivity However, the formation of shorter chain acids and other by-products requires a costly purification step that has contributed to the absence of the Cobalt acetate process in industrial production Other work on cobalt acetate systems include the efforts of Park et al ,[171] where they obtained higher conversions (~ 90%) and higher selectivity (~ 80%) by the addition of cyclohexanone The addition of the cyclohexanone also decreased the induction period from 6 hours to about 20-40 minutes [171] Cyclohexanone is more reactive toward oxidation than the cyclohexane itself The increased reactivity associated with the addition of cyclohexanone is that the cyclohexanone acts as a radical initiator and will introduce radicals into the system, therefore reducing the induction period Although higher selectivity has been obtained with the Parks system

the production of shorter chain acids requires extensive purification that hinders its industrial viability

Initial investigations in our laboratory considered deep and direct oxidation of cyclohexane to adipic acid. An efficient Fe(II) phenanthroline based catalyst has been developed that will selectively oxidize cyclohexane to cyclohexanol and cyclohexanone and reaches a maximum conversion of about 2 %. Once the conversion of cyclohexanol and cyclohexanone reach 8% the system starts to produce adipic acid. The conditions of these reactions are mild (T= 120-145 °C) and use air or oxygen as an oxidant. After our preliminary investigations the best system was found to be a neat cyclohexane with a soluble iron(II) phenanthroline catalyst with dioxygen as the oxidant.

The driving force behind this research was the potential to develop a single step synthesis for adipic acid that would rid the need to use nitric acid. As mentioned before oxidation of cyclohexanol and cyclohexanone with nitric acid produces N_2O and NO_x gases which are harmful greenhouse gases. Implementation of abatement technologies used by major producers of adipic acid has significantly reduced emissions of the harmful greenhouse gases by ca. 95 %.[172] Therefore N_2O and NO_x emission from adipic acid production is no longer a significant environmental concern

Experimental Section

Instrumentation

Gas chromatography was done on a Hewlett-Packard 5890 instrument equipped with a FID detector and a HP-INNOWax capillary column with helium as the carrier gas, or an SRI 8610 instrument equipped with a TCD detector and a Carbosieve S-II

packed column Calibration curves were used to relate peak areas of the product with the peak area of the internal standard.

Materials

Cyclohexane was purchased from Aldrich and was distilled from calcium hydride before use o-dichlorobenzene, 4 7-diphenyl 1 10 phenanthroline 2,9-dimethyl 4 7-diphenyl-1,10-phenanthrohne were purchased from Aldrich and used as received $Ru(dmdpphen)_2Cl_2$ was prepared according to a published procedure [173] $Fe(proph(C_6F_5)_4)Cl$ was purchased from Mid-Century and used as received $Fe(porph(C_6H_5)_4)Cl$ was purchased from Aldrich and used as received

Preparation of $Fe(dpphen)_3(Trf)_2$

Ten ml of 1 M $AgCF_3SO_3$ aqueous solution was added to 10 ml of 0 5 M $FeCl_2$ aqueous solution A white precipitate (AgCl) formed immediately upon the addition of the two aqueous solutions The solution was allowed to stir for three hours then filtered The filtrate which contains an aqueous solution of $Fe(CF_3SO_3)_2$ to which was then added 30 ml of an ethanolic solution 0 5 M dpphen Upon the addition of the dpphen solution the solution immediately turned dark red. The dark red solution was then allowed to stir for 3 hours uncovered which allowed the solution volume to reduce to ~ 10 ml The resulting solution contained a dark red precipitate, which was isolated and washed with small amounts of ethanol Dark red solid was then dried in vacuum oven at 65 °C for 6 hours resulting in dark red powder (yield 87 %) Anal. Calcd for

$Fe_1C_{74}H_{48}N_6O_6F_8S_2$ (%) C, 65 78, H,3 58, N, 6 22 Found (%) C, 65 66, H, 3 53, N, 6 13

Cyclohexane Oxidations with glass bottle reactor

These initial reactions were carried out in a 250 ml glass bottle reactor Reactions consisted of the following catalyst (8.8×10^{-6} mol), *o*-dichlorobenzene 10 ml (88 mmol), cyclohexane 5 ml (46 mmol), and 45 psi of air The reaction solution was placed into a constant temperature oil bath at 120 °C, stirred with a magnetic stirrer, and reaction was allowed to proceed for six hours Soluble products were analyzed by GC and adipic acid was measured by mass.

Cyclohexane Oxidations with air

Oxidations were carried out employing a 300 ml stainless steel high pressure stirred reactor (Parr Type) with a glass liner insert The reaction consisted of the following conditions: 50 ml cyclohexane (0 46 mol), 50 ml *o*-dichlorobenzene (0 44 mol) catalyst (3.5×10^{-5} mol) Each reaction was pressurized with 250 psi of air, heated to 135 °C, and the reaction was allowed to stir for six hours The reactor was cooled in an ice-bath and depressurized Reaction solution was then filtered to remove the solid adipic acid and the soluble products were monitored by GC analysis using acetophenone as an internal standard

Caution It is important to note that the combination of molecular oxygen with organic compounds at elevated temperatures is a potential explosion hazard Extreme caution should be taken in the charging and disassembly of the reaction apparatus The

use of safety shields and allowing the reaction to cool prior to disassembly is highly recommended

Cyclohexane Oxidation with O_2

Oxidations were carried out employing a 300 ml stainless steel high pressure stirred reactor (Parr Type) with a glass liner insert. The reaction consisted of the following: 50 ml cyclohexane (0.46 mol), 50 ml *o*-dichlorobenzene (0.44 mol), (or 100 ml of cyclohexane 0.92 mol), catalyst (3.5×10^{-5} mol). Each reaction was pressurized with 50 psi of O_2, and heated to 135 °C. The pressure in the reactor increased to 85 psi upon heating and this pressure was maintained with O_2 from a gas burette. Reaction was allowed to proceed until oxygen uptake had ceased. The reactor was cooled in an ice-bath and depressurized. Reaction solution was then filtered to remove the solid adipic acid and the soluble products were monitored by GC analysis using acetophenone or dichlorobenzene as an internal standard.

Results and Discussion

Cyclohexane oxidation with Air

Research performed in our laboratory by Xu[174] demonstrated that a homogeneous catalyst tris(dpphen)iron(II) (dpphen = 4,7-diphenyl-1,10-phenanthroline) will catalyze the oxidation of cyclohexane with air or oxygen as the oxidant. Initial cyclohexane oxidation experiments were conducted in a 250 ml glass bottle with *o*-dichlorobenzene as a co-solvent. *O*-dichlorobenzene (dcb) readily dissolves the metal complex and the cyclohexane (Cy), resulting in a dark red homogeneous solution. The dark red solution was then subjected to 45 psi of air and heated to 120 °C for 6 hours.

The main products of this reaction are cyclohexanol (A) and cyclohexanone (K) and adipic acid (AA) Adipic acid was deposited on the bottom of the reactor, and the solution contained a mixture of cyclohexanone and cyclohexanol at 1.2:1 ratio respectively, which results in the total isolated products equaling ~3 % conversion of cyclohexane [174] It was also observed that the is temperature sensitive with a range between 110 °C and 140 °C A reaction temperature of 130 to 135 °C was used in subsequent reactions to ensure high reactivity without catalyst deactivation

Initial studies revealed that the catalyst produced during the reaction was very reactive and experiments showed that there was no induction period Initial studies by Xu determined that oxygen was the limiting reagent in the system and perhaps the full potential of this catalyst was still unexplored Therefore, we decided to investigate the oxidation reaction on a batch scale with higher pressures of air

First set of reactions employed was to test the co-solvent dependency of the oxidation system The co-solvent dependency was tested by varying the ratio of dcb and cy while keeping the volume of the total solvent constant (Figure 4-6) Solvent composition was varied from 25 to 90% of dcb The 90% dcb solution produced only trace amounts of K and A apparently due to significant dilution of the substrate Solubility of the catalyst is somewhat limited in a solution of 25% dcb When the dcb concentration is below 25% the catalyst produces a cloudy solution but solution will become clear upon completion of the reaction The highest production of AA was observed in the 1:1 mixture of dcb and cy Therefore, the 1:1 ratio was used for the remainder of these air oxidation experiments

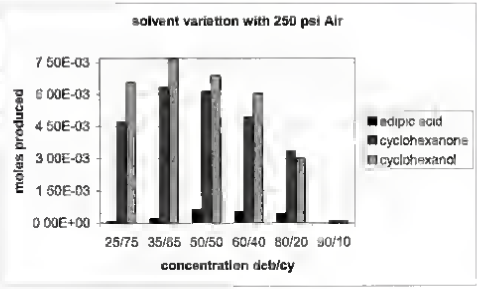

Figure 4-6. Co-solvent dependence with air as oxidant

Cyclohexane oxidation with O_2

Typical batch scale reactions consisted of the following: 50 ml of Cy, 50 ml dcb, 250 psi of air(50 psi O_2) and 3.5 x 10^{-5} mol of catalyst. Results obtained from this experiment were consistent with the results obtained from Xue ~3% total conversion of cyclohexane. The final pressure of the reactor was 200 psi, indicating that all the oxygen had been consumed during reaction. We sought to explore the full potential of this catalytic system therefore; we designed a system that would replenish the oxygen that the reaction consumes. A gas burette was constructed, which consisted of a lecture bottle, pressure regulator, pressure transducer, and a hose fitted with a check valve. Keeping the pressure constant in the reactor allowed the consumed oxygen to be monitored. Changing the system from air to pure oxygen significantly increased the amounts of all products produced. Product distribution for this reaction, shown in

Figure 4-7 reveals that the cyclohexanone (K) and cyclohexanol (A) reach a steady state concentration at about 8 % total conversion of cyclohexane with a 1 5 1 ratio respectively

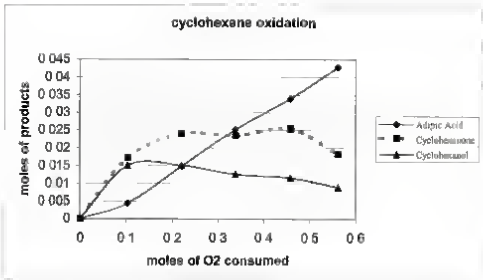

Figure 4-7 Product Distribution catalyzed by $Fe(dpphen)_3Trf_2$ in 50ml dcb 50ml cy

Each set of data points in Figure 4-7 represents a run where an initial charge of catalyst (3.0×10^{-5} mol) was introduced into 100 ml of total solution The reaction mixture was then heated to 135 °C and allowed to proceed until oxygen uptake had ceased The cooled reaction solution was filtered to remove the solid adipic acid and the filtrate returned to the reactor with additional cyclohexane to make up for any loss This process was repeated five times without any loss of reactivity Oxygen uptake rates for each of the five runs are depicted in Figure 4-8

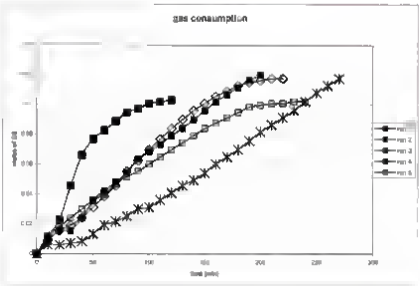

Figure 4-8. Oxygen uptake rates for $Fe(dpphen)_3Trf_2$ in 50 ml deb / 50 ml of Cy

The initial run has the highest rate of oxygen consumption with 1.3×10^{-3} mol O_2 / min with most of the oxygen being consumed in the first hour. Run 2 was significantly slower than the other runs with a rate of 4.0×10^{-4} mol O_2 / min. The rapid uptake in the first run may be due to the activation of the catalyst precursor. The uptake rate slows at the end of the first run and continues into the second run. Runs 3, 4, and 5 have consistent rates with an average rate of 6.5×10^{-4} mol O_2 / min. A higher concentration of the more easily oxidized K may contribute to the overall rate enhancement of the later runs. Figure 4-8 indicates that in the later runs the uptake of oxygen stops abruptly. This sudden interruption of oxygen flow is probably due to the production of CO and CO_2 gases. The CO_2 and CO gases are produced as result of the complete combustion of the cyclohexane. Production of these gases will displace the oxygen in the reactor headspace and not allow the consumed oxygen to be replaced. Analysis of

the oxygen equivalents that are present in the isolated products (oxygen efficiency) supports the theory of over oxidation. Oxygen efficiency in the first two runs are 35 and 30% respectively while the later runs yield 18-22 % efficiency indicating that more of the product is being over oxidized.

$$\xrightarrow{O_2} \quad 5\,CO_2 \;+\; CO \;+\; 6\,H_2O$$

Catalyst Variation

It is of interest to compare the general reactivity of different catalyst formulations and different catalyst structures Complexation of the anion does not appear to be associated the active catalyst either Experiments designed to examine the effects that counterion coordination has on reactivity, revealed that there was no reactivity dependence associated with the coordinating ability of the anion [174]

Table 4-1. Ligand variation of iron catalysts[a]

Catalyst	% conversion	AA / 10^{-3} mol	K / 10^{-3} mol	A / 10^{-3} mol	TO[b]	time (min)
Fe(dpphen)$_3$Trf$_2$	8 0	4 38	17 2	15 0	1045	120
Fe(dmdpphen)$_3$Trf$_2$	9 1	8 9	20 0	13 0	1197	340
Fe(proph(C$_6$F$_5$)$_4$)Cl	4 7	0 93	11 2	9 5	618	280
Fe(porph(C$_6$H$_5$)$_4$)Cl	5 1	0 006	9 3	14 2	672	320

[a] Ligand variation experiments were carried out in a 300 ml stirred stainless steel autoclave with 3 5 x 10^{-5} mol of catalyst in *o*-dichlorobenzene (50 ml) and cyclohexane (50 ml 46 mmol) The catalyst solution was then charged with 50 psi of oxygen and the pressure was held constant at 80 psi after heating Reactions were allowed to proceed until oxygen uptake had ceased. Fe(porph(C$_6$F$_5$)$_4$)Cl = tetra(pentafluorophenyl)porphyrin- Iron(III)chloride. Fe(porph(C$_6$H$_5$)$_4$)Cl = 5,10,15,20-Tetraphenylporphyrin Iron(III) chloride

The activity of $[Fe(dpphen)_3](CF_3SO_3)_2$ was also compared to other well known alkane oxidation catalysts and other Fe(II) complexes with different nitrogen containing ligands (Table4-1). A number of nitrogen containing ligands were tested as iron(II) complexes under our oxidative conditions (50 psi of O_2 and 135 °C in a 1:1 mixture of dcb and cyclohexane). Interestingly only ligands with a phenyl group substituted in the 4,7, and 4,4' of phenanthroline and 2,2'-bipyridyl respectively showed activity toward oxidation of cyclohexane. Phenyl substituents apparently offer added solubility that increases catalyst solubility and allow for homogeneous oxidation to occur. Iron porphyrin catalysts have been shown to have remarkable activity for the oxidation of hydrocarbons[175-177] and peroxide decomposition catalysts [178] We subjected iron porphyrin complexes to the oxidative conditions of our system and found them to be somewhat less reactive than our current catalyst system.

Solvent variation with O_2

We decided to revisit the solvent dependency experiments considering that different behavior was observed with an unlimited supply of oxygen. The solvent ratio was varied from 90 % dcb to 100 % cyclohexane. Analysis of the data obtained from these experiments (Figure 4-9) revealed that the product distribution was approximately the same for each solvent composition. These results were surprising considering that the catalyst precursor is not soluble in solutions with less than 20% dcb. Reactions with 20 % dcb or less produced a cloudy solution or a suspension of the catalyst. A homogeneous solution was obtained after heating the reaction solution to 135 °C with oxygen pressure. The 50/50 solvent mixture produced the highest conversion of

cyclohexane with 9 3% The persent conversions of the other solvent mixtures were around 5% with the exception of the 30/70 solution having a conversion of 6 7%

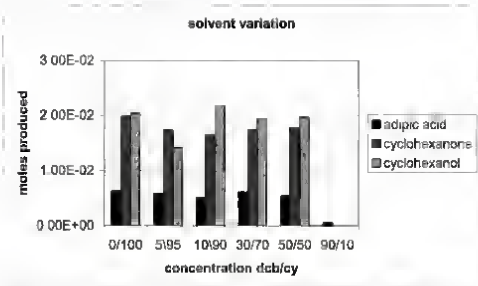

Figure 4-9 Solvent variation with constant oxygeo system

Neat cyclohexane oxidation

Considering the benefits that a single component system offers over the co-solvent system, subsequent experiments were performed in neat cyclohexane. Despite the initial insolubility of the starting iron complex in neat cyclohexane there is still no induction period associated this catalytic system Initially the iron complex is a red suspension in cyclohexane, but once the reaction medium was heated to temperature under oxygen pressure the catalytic mixture was transformed into a homogeneous light yellow solution. Reactivity of this neat cyclohexane solution is different from the 1 1 co-solvent mixture in that the steady state concentration of the cyclohexanol is nearly

doubled in the neat cyclohexane system. The oxygen uptake rates in neat cyclohexane for the first three runs are 5.0×10^{-4}, 4.0×10^{-4}, 6.0×10^{-4} mol O_2 / min respectively (figure 4-10). These rates are in line with the co-solvent system with the exception of the first run, where the catalyst precursor must first undergo a transformation to go into solution resulting in lower initial activity.

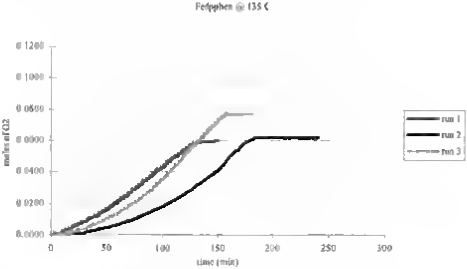

Figure 4-10. Oxygen uptake rates for $Fe(dpphen)_3Trf_2$ in 100 ml cyclohexane, T= 135 °C

The neat cyclohexane system is also more efficient than the co-solvent system where 74% of the oxygen consumed in the first run can be accounted for in the three major products. Production of the over oxidation products is more apparent in this system because of the sudden stop in the oxygen consumption. This sudden stop in oxygen uptake is presumed to be a result from the higher concentration of the more easily oxidized products, which in turn undergoes complete oxidation to CO, CO_2, and H_2O. Figure 4-10 represents uptake rates for three runs in neat cyclohexane at 135 °C.

Analysis of the product formation reveals that cyclohexanone reaches a steady state concentration 3 7 x 10^{-1} M approximately 4% of the total cyclohexane solution Cyclohexanol also reaches a steady state concentration at 2 4 x 10^{-1} M or 2 6% of the total cyclohexane solution Analysis of the product formation data reveals that adipic acid is responsible for the production of CO and CO_2 Figure 4-11 represents the rate of product formation compared to the rate of O_2 uptake for the first three runs. The graphs reveal that the system is most efficient when building the concentrations of the K and A. Once the intermediates reach their peak concentrations and the adipic acid becomes the major new product being formed and the production of the over oxidation products CO and CO_2 increase. This trend is clear from the analysis of the data in figure 4-12 where at the start of the reaction the only gases that are present is O_2 and N_2 and as the reaction progresses the O_2 level decreases and CO and CO_2 replace the volume once occupied by the O_2

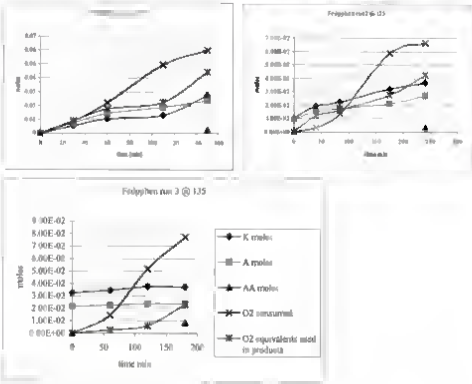

Figure 4-11: Product formation data from Cyclohexane solution with $Fe(dpphen)_3Trf_2$ and Oxygen at 135 °C

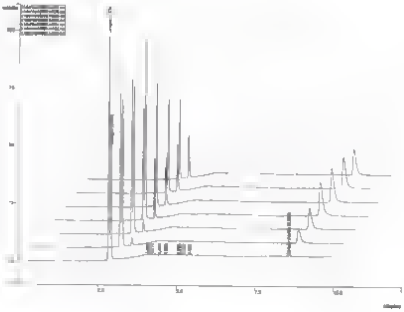

Figure 4-12. Head gas composition from the reaction of cyclohexane solution with $Fe(dpphen)_3Tf_2$ and Oxygen at 135 °C

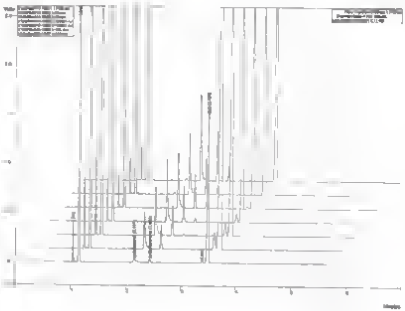

Figure 4-13. GC overlay of the reaction with cyclohexane solution with $Fe(dpphen)_2Trf_2$ and Oxygen at 135 °C

Conclusion

An alternative catalyst system has been developed for the selective oxidation of cyclohexane to cyclohexanol and cyclohexanone. The catalyst used is an iron(II) phenyl substituted phenanthroline complex that will catalyze the oxidation of cyclohexane under mild conditions. The presence of phenyl substituents on the ligands of the catalyst increases its solubility in hydrocarbon solvent and allows for the oxidation to proceed smoothly at mild temperatures. Comparing the reactivity of the $Fe(dpphen)_2OTF_2$ to the heterogeneous system developed by Thomas[166] our system is significantly more reactive, where 8% of the cyclohexane is oxidized in 1-3 hours versus 3-4% of the

cyclohexane is oxidized in 15 –20 hours by Thomas s system Our system is also much milder than the Tanaka[170] system because there is no additional oxidant used to facilitate the oxidation and the catalyst charge is 10 times more than our system Tanaka's system converts cyclohexane up to 80% but requires acetic acid as a solvent. Although our system only converts about 8% of the cyclohexane it is a much cleaner and milder process

Chapter 5

HYDROCARBON OXIDATION WITH A GIF-TYPE CATALYST

Introduction

Selective oxidation of hydrocarbon substrates is of considerable importance and has been focus of intense research for many years.[179-181] Cyclohexane oxidation has been of particular interest in our laboratory in recent years. As discussed in chapter 4 the employment of iron(II) phenanthroline catalysts will selectively oxidize cyclohexane to cyclohexanol and cyclohexanone. Conversion of the reaction is limited to about 8% due to increased concentration of the more reactive products that can more easily undergo complete oxidation to produce CO_2 and H_2O. Ligands employed for this catalytic system are phenyl-substituted phenanthroline type ligands, which have a significant cost associated with them. The phenyl substitution on the phenanthroline is required for the resultant catalyst to be active in our system. The significant cost of the ligand prompted us to investigate other ligands that offered the same solubility as the phenanthroline based catalysts, but not have the cost associated with them. Our search led us to the Gif-type systems developed by Barton and co-workers.[182-184]

Barton's systems are composed of an $Fe^{II/III}$ complex, a peroxide (t-butylperoxide or hydrogen peroxide) in a pyridine-carboxylic acid solution (10:1 v/v).[185] This reaction mixture selectively affords nearly quantitative yields of ketones

with conversions up 20-30 % at room temperature or below Gif-type chemistry involves the formation of an Fe^{+3}-OOH species that eliminates H_2O and produces an Fe^{+5}=O species (figure 5-1) [186]

$$Fe^{+3}\text{——}O\text{—}OH \longrightarrow Fe^{+5}\text{=}O + H_2O \qquad \textbf{Fig 5 1}$$

This reaction sequence is said to involve an Fe^{+3}-Fe^{+5} manifold [187] The reactivity of the 3-5 manifold does not involve carbon centered radicals [188] On the contrary, there is a second manifold based on Fe^{+2}-Fe^{+4} chemistry does involve carbon radicals.[188] Both systems selectivity oxidize saturated hydrocarbons at the secondary position.[190] The Fe^{+3} carboxylate catalysts utilized in Gif chemistry may be an attractive alternative catalyst composition to be employed in our catalytic system

Conditions of the Gif system are extremely different from the conditions employed in our system. A high concentration of pyridine and acetic acid (or other acid) is necessary for Gif chemistry to take place Here we report our results on cyclohexane oxidations using the analogous catalysts and show the system will oxidize cyclohexane without the use of added peroxide

Experimental

Materials Trimethylacetic acid, $FeCl_2 4H_2O$ and $FeCl_3$ was purchased form acros and used as received All solvents were purchased from Aldrich and distilled prior to use. $Fe_3O(tmn)_6L_2$ was prepared according to a published procedure [185]

Oxidation methods Oxidation reactions were carried out in a 300 ml stainless steel autoclave The autoclave was equipped with the following: thermocouple, magnetic

drive stirrer, gas entrainment stirrer stainless steel sampling tube, glass insert the glass insert was capped with a Teflon wafer to minimized contact with the stainless steel surface. A Small amount of cyclohexane was added to the outside of the liner to ensure good thermal contact. The catalyst (3.5×10^{-5} mol) was dissolved in a total of 100 ml of cyclohexane 40 psi of oxygen was added to the stirred solution before heating. Solution was then heated to the specified temperature and the final pressure was maintained with a gas burette filled with oxygen. Oxygen consumption was monitored with a pressure transducer and a digital data recorder Reaction solution was sampled at various times After the specified reaction time, the reactor was then cooled to room temperature, gasses were slowly released into the atmosphere and reaction apparatus was disassembled Reaction solution was then filtered to remove the solid product and the liquid products were monitored via gas chromatography with o-dichlorobenzene as an internal standard

Results and Discussion

The desire to find cheaper ligands that will perform the oxidation of cyclohexane has led us to employ the trimethylacetate ligand (tma) Reasons for choosing the tma ligand is due to the large bulky aliphatic groups of the trimethylacetate make the iron complex very soluble in hydrocarbon solvent The Fe(tma) complex has the general formula of $Fe_3O(Piv)_6L_3$ where Piv = O_2CCMe_3 and L = pyridine, Hpiv, H_2O The Fe(tma) complex employed in Gif chemistry required a high concentration of pyridine, peroxide, and relatively low temperature (50 °C) The conditions of our system, removed the added oxidant (no added peroxide), decreased the catalyst concentration to 3.5×10^{-5} mol and increased reaction temperature to 130-145 °C.

The reactivity of the catalyst was absent when the capping ligands (L) were H_2O or Hpiv. Similar to Gif systems, we found that pyridine is a necessary ligand (L) for the complex to be active. When L= pyridine the catalyst showed significant reactivity. The formation of the pyridine adduct can be performed in-situ or prior to reaction.

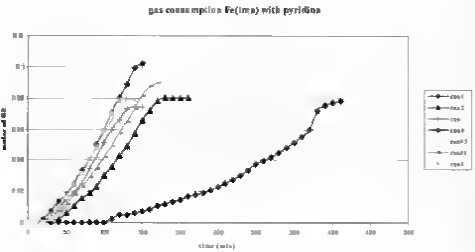

Figure 5-2 Oxygen uptake experiments for Fe(tma)py catalyst system. Reaction conditions: 100 ml Cyclohexane (0.92 mol), 3.5×10^{-5} mol of Fe(tma), 2.5×10^{-4} mol of pyridine, temperature = 135 °C, 40 psi of oxygen at room temperature. Heating of the reaction solution increased the internal pressure to 80 psi. The pressure in the reactor was maintained with a gas burette and the oxygen consumption was monitored.

Figure 5-2 depicts a significant induction period (~90 min) associated with the catalytic mixture. The induction period may be linked to loss of one of the pyridine ligands that caps each iron of the tri-iron complex. Mass spec studies confirms that the tri-iron complex will lose the capping ligands of as the reaction temperature increases (figure 5-3). The temperature of the mass spec capillary does not necessarily correspond

to the temperature of the reaction solution. It appears that once the complex loses one of its capping ligands the metal species becomes reactive.

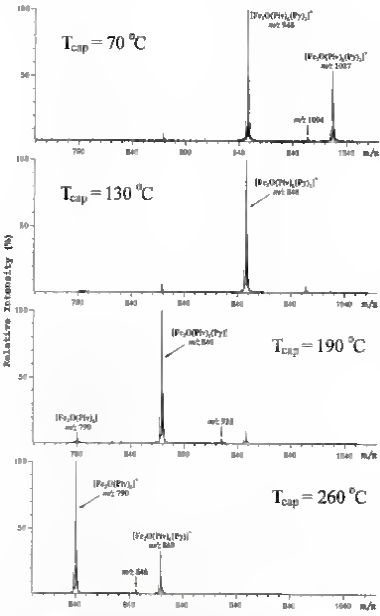

Figure 5-3 Mass spec of $Fe_3O(Piv)_6(Py)_3$ at different capillary temperatures. An electrolyte was added to the solution to oxidize the complex to an overall +1 charge.

Considering that the induction period may be associated with the loss of a pyridine capping ligand it stands to reason that increasing the reaction temperature may shorten the induction period The reaction temperature was increased to 145 °C and the induction period was reduced to less than 10 minutes (figure 5-4) The oxygen uptake rate for the first run is 4.0×10^{-4} mol of O_2 min^{-1} This rate is comparable to the iron(II) phenanthroline catalysts (6.0×10^{-4}) at the corresponding temperature

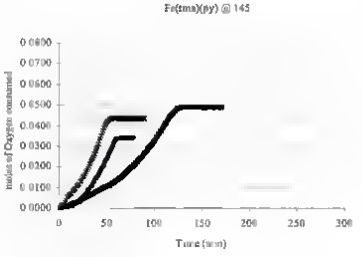

Figure 5-4 Oxygen uptake rates for Fe(tmtu)(py) in neat cyclohexane and 145 °C

Time dependent studies of the formation of oxygenated products are illustrated in figure 5 6 The moles of oxygen consumed is the amount of oxygen that the reaction actually consumed from the burette, it does not take into account the amount of oxygen added to the reactor initially Major products of the reaction are cyclohexanone (K)

cyclohexanol (A), and adipic acid. The total products curve represents the number of oxygen equivalents accounted for by the reaction products. Analysis of the data in figure 5-5 reveals that the catalyst mixture is efficient in converting the cyclohexane into the major products K and A. The system with Fe(tma)(py) is similar to the Fe(II)/pphen system where the later runs of the reaction produce more of the higher oxidation products CO_2 and water. Figure 5-6 depicts the products and the oxygen consumed against one another and reveals that most of the oxygen consumed in the reaction cannot be accounted for in the main isolated products.

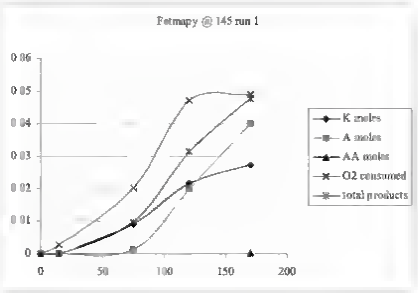

Figure 5-5. Product distribution for Fe(tma)(py) in neat cyclohexane at 145 °C, first run.

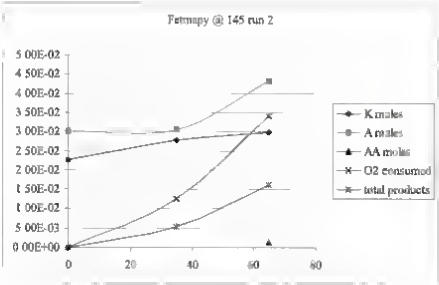

Figure 5-6. Product distribution for Fe(tma)(py) in neat cyclohexane at 145 °C, second run

Comparison to the Gif systems our catalyst reactivity is considerably different than those obtained by Barton and co-workers. Barton's catalytic mixture produced an almost quantitative yield of K [102,191]. Figure 5-5 reveals that the (K) is the dominating product initially, but (A) soon takes over and is the dominant species in solution after reaction is complete.

Generally, there are two types of mechanisms that one must consider for the oxidation of hydrocarbons. The first type suggests that the C-H bond cleavage is a result of the interactions of the substrate with the metal center. Second type of mechanism suggests that the C-H bond cleavage is caused by a metal free species ($HO^{\bullet}$, $RO^{\bullet}$, etc.) and the role of the catalyst is in the generation of the reactive species. The ratio of

products is K.A is 1 1 4 and the mechanism can probably be best described as a peroxide decomposition catalyst figure 5 7

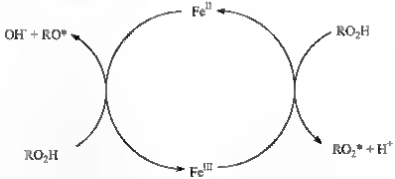

Figure 5-7 Catalytic peroxide decomposition by an iron(II), iron(III) catalyst

One important aspect of this oxidation chemistry is that the catalyst needs to be able to shuttle back and fourth between oxidation states This can be seen in the above diagram where the role of the catalyst is in the decomposition of the alkyl peroxide. The above mechanism would suggest that if the catalyst can shuttle between the +2 and +3 oxidation state the product ratio should be about the same This mechanism and the product distribution obtained from the reaction supports that the catalyst functions in that manner

Conclusion

The quest for finding a cheaper catalyst was achieved with the Fe(tma)(py) complex There are many similarities between the iron(II) phenanthroline and the Fe(tma)(py) complex when the temperature is raised to 145 °C. The main difference in the two catalytic systems is that the Fe(tma)(py) complex is somewhat slower and less reactive

APPENDIX A
TABLES OF CRYSTALLOGRAPHIC DATA

This appendix contains the tables of crystallographic data for the structure determination of compound **2-6**

Table 1 Crystal data and structure refinement for **2-6**

Identification code	kw05	
Empirical formula	C52 H51 B Cl2 F19 Li O2 Si Zr	
Formula weight	1276 89	
Temperature	173(2) K	
Wavelength	0 71073 Å	
Crystal system	Monoclinic	
Space group	P2(1)/c	
Unit cell dimensions	a = 9 7946(4) Å	□= 90°
	b = 34 502(1) Å	□= 102 985(1)°
	c = 16 8584(7) Å	□ = 90°
Volume	5551 4(4) Å^3	
Z	4	
Density (calculated)	1 528 Mg/m^3	
Absorption coefficient	0 419 mm^{-1}	
F(000)	2584	
Crystal size	0 26 x 0 12 x 0 08 mm^3	
Theta range for data collection	1 71 to 27 50°	
Index ranges	-12 ≤ h ≤12, -44 ≤ k ≤0, -18 ≤ l ≤21	
Reflections collected	50496	
Independent reflections	12707 [R(int) = 0 0821]	
Completeness to theta = 27 50°	99 6 %	
Absorption correction	Integration	
Max and min transmission	0 9686 and 0 9055	
Refinement method	Full-matrix least-squares on F^2	
Data / restraints / parameters	12707 / 0 / 727	
Goodness-of-fit on F^2	1 008	
Final R indices [I>2sigma(I)]	R1 = 0 0531, wR2 = 0 1166 [7452]	
R indices (all data)	R1 = 0 1114, wR2 = 0 1430	
Extinction coefficient	0 00040(15)	

Largest diff peak and hole 0 584 and -0.743 e.Å^{-3}

R1 = □(||F_o| - |F_c||) / □|F_o|

wR2 = [□□w(F_o^2 - E_c^2)^2] / □□wF_o^{22}]]$^{1/2}$

S = [□□w(F_o^2 - F_o^2)^2] / (n-p)]$^{1/2}$w= 1/[□^{2}(F_o^2)+(0 0370*p)^2+0.31*p], p = [max(F_o^2,0)+ 2* F_c^2]/3

Table 2 Atomic coordinates (x 10^4) and equivalent isotropic displacement parameters (Å^{2}x 10^3)
for kw05 U(eq) is defined as one third of the trace of the orthogonalized U^{ij} tensor

	x	y	z	U(eq)
Zr	1518(1)	4129(1)	13001(1)	26(1)
Cl1	3159(1)	3733(1)	13973(1)	41(1)
Cl2	-558(1)	3820(1)	13381(1)	37(1)
B	6105(4)	3823(1)	8581(3)	25(1)
St	4755(1)	3877(1)	12155(1)	27(1)
C15	5532(4)	3431(1)	12695(2)	38(1)
C16	5637(4)	4293(1)	12762(2)	38(1)
C1	2751(5)	4645(1)	13956(3)	46(1)
C2	2512(5)	4795(1)	13169(3)	44(1)
C3	1050(5)	4841(1)	12877(3)	38(1)
C4	409(5)	4712(1)	13496(3)	37(1)
C5	1447(5)	4590(1)	14157(3)	41(1)
C6	2783(4)	3910(1)	11969(2)	28(1)
C7	1792(4)	3605(1)	12003(2)	27(1)
C11	2115(4)	3190(1)	12239(3)	37(1)
C8	426(4)	3751(1)	11712(2)	31(1)
C12	-915(4)	3524(1)	11559(3)	39(1)
C9	528(4)	4146(1)	11486(2)	31(1)
C13	-685(4)	4397(1)	11081(3)	43(1)
C10	1989(4)	4239(1)	11608(2)	27(1)
C14	2531(4)	4598(1)	11281(2)	33(1)

C17	5146(4)	3876(1)	11101(2)	25(1)
C18	5830(4)	4190(1)	10717(2)	27(1)
F1	5875(2)	4535(1)	11102(1)	35(1)
C19	5887(4)	4161(1)	9946(2)	25(1)
F2	6354(2)	4485(1)	9636(1)	31(1)
C20	5694(4)	3825(1)	9477(2)	24(1)
C21	5246(4)	3515(1)	9875(2)	27(1)
F3	5058(2)	3160(1)	9526(1)	35(1)
C22	4946(4)	3543(1)	10634(2)	27(1)
F4	4425(3)	3224(1)	10930(1)	41(1)
C23	7816(4)	3878(1)	8827(2)	25(1)
C24	8642(4)	3584(1)	9278(2)	29(1)
F5	8006(2)	3250(1)	9427(1)	37(1)
C25	10067(4)	3603(1)	9570(2)	30(1)
F6	10787(2)	3308(1)	9990(2)	45(1)
C26	10783(4)	3933(1)	9442(2)	32(1)
F7	12157(2)	3960(1)	9746(2)	48(1)
C27	10031(4)	4235(1)	9019(2)	32(1)
F8	10682(2)	4565(1)	8897(2)	47(1)
C28	8589(4)	4200(1)	8727(2)	28(1)
F9	7964(2)	4512(1)	8315(1)	36(1)
C29	5612(4)	3428(1)	8049(2)	29(1)
C30	4209(4)	3309(1)	7907(2)	33(1)
F10	3309(2)	3511(1)	8247(1)	41(1)
C31	3656(5)	3000(1)	7423(3)	44(1)
F11	2301(3)	2902(1)	7338(2)	63(1)
C32	4508(6)	2791(1)	7047(3)	50(1)
F12	3985(4)	2489(1)	6553(2)	77(1)
C33	5889(5)	2890(1)	7142(3)	47(1)
F13	6714(4)	2890(1)	6761(2)	79(1)
C34	6409(4)	3203(1)	7837(3)	37(1)
F14	7768(3)	3281(1)	7687(2)	47(1)
C35	5266(4)	4165(1)	7959(2)	27(1)
C36	5596(4)	4222(1)	7207(2)	30(1)
F15	6681(2)	4021(1)	7031(1)	38(1)
C37	4891(4)	4461(1)	6606(2)	32(1)

F16	5267(3)	4497(1)	5888(1)	48(1)
C38	3752(4)	4664(1)	6738(2)	35(1)
F17	3005(3)	4898(1)	6148(2)	52(1)
C39	3365(4)	4624(1)	7469(2)	35(1)
F18	2248(3)	4821(1)	7594(2)	53(1)
C40	4113(4)	4375(1)	8049(2)	30(1)
F19	3604(2)	4349(1)	8725(1)	41(1)
Li	-288(9)	3489(2)	14668(4)	46(2)
O1	202(4)	2951(1)	14565(2)	61(1)
C41	680(8)	2802(2)	14043(4)	83(2)
C42	204(10)	2567(2)	13333(4)	130(4)
C43	1965(8)	2625(2)	14530(5)	113(3)
C44	-941(6)	2660(2)	14945(3)	65(2)
C45	-592(7)	2708(2)	15837(3)	90(2)
C46	-2528(6)	2673(2)	14605(4)	89(2)
O2	513(3)	3827(1)	15534(2)	35(1)
C47	640(4)	3937(2)	16194(3)	43(1)
C48	370(5)	3823(2)	17009(3)	67(2)
C49	1922(5)	3738(2)	16027(3)	48(1)
C50	-1808(4)	4045(1)	15487(3)	38(1)
C51	-2980(5)	3787(2)	15072(3)	59(1)
C52	-1776(5)	4420(1)	15044(3)	52(1)

Table 3 Bond lengths [Å] and angles [°] for **2-6**

Zr-Cl1	2.4407(11)
Zr-C6	2.472(3)
Zr-C2	2.485(4)
Zr-C3	2.499(4)
Zr-Cl2	2.5033(10)
Zr-C4	2.514(4)
Zr-C1	2.517(4)
Zr-C9	2.522(4)
Zr-C10	2.522(4)
Zr-C7	2.525(4)
Zr-C5	2.528(4)
Zr-C8	2.555(4)
Cl2-Li	2.415(8)
Si-C29	1.642(6)
Si-C23	1.644(5)
Si-C20	1.648(5)
Si-C35	1.667(6)
Si-C16	1.861(4)
Si-C15	1.861(4)
Si-C6	1.889(4)
Si-C17	1.900(4)
C1-C2	1.396(6)
C1-C5	1.406(6)
C2-C3	1.415(6)
C3-C4	1.405(5)
C4-C5	1.394(6)
C6-C10	1.432(5)
C6-C7	1.442(5)
C7-C8	1.410(5)
C7-C11	1.500(5)
C8-C9	1.424(6)
C8-C12	1.501(5)
C9-C10	1.436(5)
C9-C13	1.504(6)

C10-C14	1 499(5)
C17 C22	1.382(5)
C17 C18	1 397(5)
C18-F1	1 352(4)
C18-C19	1.380(5)
C19-F2	1 359(4)
C19-C20	1 392(5)
C20 C21	1.386(5)
C21 F3	1 353(4)
C21 C22	1.379(5)
C22-F4	1 355(4)
C23-C28	1 376(5)
C23-C24	1 409(5)
C24-F5	1 359(4)
C24 C25	1 374(5)
C25 F6	1 337(4)
C25-C26	1 369(6)
C26 F7	1 349(4)
C26-C27	1 373(6)
C27-F8	1 342(4)
C27-C28	1 393(5)
C28-F9	1 351(4)
C29-C34	1 394(5)
C29-C30	1 403(5)
C30-F10	1 349(4)
C30-C31	1 379(6)
C31-F11	1 346(5)
C31-C32	1 362(7)
C32-C33	1 349(7)
C32 F12	1 359(5)
C33-F13	1 347(5)
C33-C34	1 394(6)
C34-F14	1 343(5)
C35 C40	1 378(5)
C35-C36	1 391(5)
C36 F15	1 356(4)

C36-C37	1 367(5)
C37-F16	1 349(4)
C37-C38	1 377(6)
C38-F17	1.361(4)
C38-C39	1.374(6)
C39-F18	1.343(4)
C39-C40	1 384(5)
C40-F19	1.345(4)
Li-O1	1 863(8)
Li-O2	1 921(8)
O1-C44	1 433(6)
O1-C41	1 502(6)
C41-C43	1 473(9)
C41-C42	1 540(9)
C44-C45	1 476(7)
C44-C46	1 531(8)
O2-C47	1 447(5)
O2-C50	1 461(5)
C47-C48	1 508(6)
C47-C49	1 512(6)
C50-C51	1 496(6)
C50-C52	1 498(6)

Cl1-Zr-C6	86 69(10)
Cl1-Zr C2	105 06(12)
C6-Zr-C2	96 73(14)
Cl1-Zr C3	133 48(11)
C6-Zr-C3	110 71(13)
C2-Zr-C3	32 98(14)
Cl1 Zr Cl2	92 28(4)
C6-Zr-Cl2	127 90(10)
C2 Zr Cl2	133 21(10)
C3 Zr-Cl2	107 22(10)
Cl1 Zr C4	119 62(10)
C6-Zr-C4	143 19(14)
C2-Zr C4	53 93(14)

C3-Zr-C4	32 56(13)
Cl2 Zr-C4	79 61(10)
Cl1-Zr-C1	79 49(12)
C6-Zr C1	114 98(14)
C2-Zr-C1	32 40(15)
C3-Zr C1	54 00(15)
Cl2-Zr-C1	115 97(11)
C4-Zr-C1	53 45(15)
Cl1-Zr-C9	137 56(10)
C6-Zr-C9	55 44(12)
C2 Zr-C9	98 40(15)
C3-Zr C9	82.63(14)
Cl2 Zr-C9	96 83(9)
C4-Zr-C9	102 80(14)
C1 Zr-C9	130 73(15)
Cl1-Zr-C10	118 59(9)
C6-Zr-C10	33 31(12)
C2-Zr Cl0	79.54(14)
C3-Zr C10	80 98(13)
Cl2-Zr-C10	129 11(9)
C4-Zr-C10	111 84(13)
C1-Zr-C10	109 17(14)
C9-Zr-C10	33 07(12)
Cl1-Zr-C7	83 87(9)
C6-Zr-C7	33 52(12)
C2 Zr-C7	129 77(13)
C3 Zr C7	133 88(13)
Cl2-Zr-C7	94 54(9)
C4-Zr C7	155 76(14)
C1 Zr-C7	145 53(14)
C9-Zr-C7	54.20(13)
C10-Zr-C7	54 38(12)
Cl1-Zr C5	87 90(11)
C6-Zr C5	147 20(14)
C2-Zr C5	53 81(14)
C3 Zr C5	53 85(14)

Cl2 Zr-C5	84 61(11)
C4-Zr-C5	32 11(14)
C1-Zr-C5	32.36(14)
C9-Zr-C5	134 12(14)
C10-Zr-C5	131 79(14)
C7 Zr C5	171 68(14)
Cl1-Zr-C8	111 79(10)
C6-Zr-C8	54 88(12)
C2-Zr-C8	130 32(14)
C3-Zr-C8	113 40(14)
Cl2-Zr-C8	77 93(8)
C4-Zr-C8	124 12(14)
C1-Zr-C8	162.54(14)
C9-Zr-C8	32 56(13)
C10-Zr-C8	54.07(12)
C7-Zr-C8	32 22(12)
C5-Zr C8	153 94(14)
Li-Cl2-Zr	120 0(2)
C29-B-C23	113 0(3)
C29-B-C20	113 7(3)
C23-B-C20	102 3(3)
C29-B-C35	101 6(3)
C23-B-C35	114 1(3)
C20-B-C35	112 7(3)
C16-Si C15	106 3(2)
C16-Si-C6	112.06(18)
C15 Si-C6	114 97(19)
C16-Si-C17	110 45(18)
C15 Si-C17	108 07(17)
C6-Si C17	104 95(16)
C2-C1-C5	108 2(4)
C2-C1-Zr	72 5(2)
C5-C1-Zr	74 2(3)
C1-C2-C3	108 2(4)
C1-C2 Zr	75 1(3)
C3-C2-Zr	74 0(2)

C4-C3-C2	107 0(4)
C4-C3-Zr	74 3(2)
C2-C3-Zr	73 0(3)
C5 C4-C3	108 8(4)
C5-C4-Zr	74 5(2)
C3 C4-Zr	73 1(2)
C4-C5-C1	107 8(4)
C4-C5-Zr	73 4(2)
C1 C5 Zr	73 4(2)
C10-C6-C7	106 7(3)
C10-C6-Si	123 8(3)
C7-C6-Si	128 4(3)
C10-C6-Zr	75.3(2)
C7 C6-Zr	75.29(19)
Si-C6-Zr	123 87(18)
C8 C7-C6	108 7(3)
C8 C7-C11	124 0(4)
C6 C7-C11	127 1(3)
C8 C7-Zr	75 1(2)
C6-C7-Zr	71 2(2)
C11-C7-Zr	123 6(3)
C7-C8-C9	108 4(3)
C7-C8-C12	126 8(4)
C9-C8-C12	124 4(4)
C7-C8 Zr	72 7(2)
C9-C8-Zr	72 4(2)
C12-C8 Zr	126 5(2)
C8-C9-C10	107 7(3)
C8-C9-C13	125 2(4)
C10-C9-C13	126 6(4)
C8-C9-Zr	75 0(2)
C10 C9-Zr	73 5(2)
C13 C9-Zr	123 9(3)
C6-C10-C9	108 2(3)
C6-C10-C14	127 3(3)
C9-C10-C14	123 8(4)

C6-C10-Zr	71 4(2)
C9-C10-Zr	73 4(2)
C14-C10-Zr	128.3(3)
C22-C17-C18	113 5(3)
C22-C17-Si	120 1(3)
C18 C17-Si	126 4(3)
F1 C18-C19	117 7(3)
F1-C18-C17	120 1(3)
C19-C18-C17	122.2(4)
F2-C19-C18	116 8(3)
F2 C19-C20	118 8(3)
C18-C19-C20	124 4(3)
C21-C20-C19	112 6(3)
C21-C20-B	127 6(3)
C19-C20-B	119 6(3)
F3 C21 C22	115 5(3)
F3-C21-C20	121 0(3)
C22-C21-C20	123.5(4)
F4-C22-C21	117 4(3)
F4-C22-C17	118 9(3)
C21-C22-C17	123 7(3)
C28-C23-C24	112 5(3)
C28-C23-B	128.3(3)
C24-C23-B	118 9(3)
F5-C24-C25	116 4(3)
F5-C24-C23	118 6(3)
C25-C24-C23	125 0(4)
F6-C25-C26	120 1(4)
F6-C25 C24	120 8(4)
C26 C25-C24	119 0(4)
F7 C26-C25	119 8(4)
F7-C26 C27	120 6(4)
C25 C26-C27	119 6(4)
F8 C27-C26	120 9(4)
F8-C27-C28	120 0(4)
C26-C27-C28	119 1(4)

F9-C28-C23	120 5(3)
F9-C28-C27	114 7(3)
C23-C28-C27	124 8(4)
C34-C29-C30	112 8(4)
C34-C29-B	127 4(3)
C30-C29-B	119 5(3)
F10-C30-C31	116 4(4)
F10-C30-C29	119 0(4)
C31-C30-C29	124 6(4)
F11-C31-C32	120 7(4)
F11-C31-C30	120 3(4)
C32-C31-C30	119 0(4)
C33-C32-F12	119 5(5)
C33-C32 C31	120 2(4)
F12-C32-C31	120 2(5)
F13-C33-C32	120 7(4)
F13-C33-C34	119 4(4)
C32-C33 C34	119 9(4)
F14-C34-C29	120 9(4)
F14-C34-C33	115 6(4)
C29-C34-C33	123 5(4)
C40-C35 C36	113 0(3)
C40-C35 B	127 1(3)
C36-C35 B	119 3(3)
F15-C36-C37	115 9(3)
F15-C36-C35	118 8(3)
C37-C36-C35	125 3(4)
F16-C37 C36	121 8(4)
F16-C37 C38	119 5(4)
C36-C37-C38	118 7(4)
F17-C38-C39	120 2(4)
F17-C38-C37	120 4(4)
C39-C38-C37	119 4(4)
F18-C39 C38	119.3(4)
F18-C39-C40	121.6(4)
C38-C39 C40	119 1(4)

F19-C40-C35	121 9(3)
F19-C40-C39	113 7(3)
C35-C40-C39	124 4(4)
O1-Li-O2	133 0(4)
O1-Li-Cl2	112 9(3)
O2 Li-Cl2	112 8(4)
C44-O1-C41	115 4(4)
C44-O1-Li	129 7(4)
C41-O1-Li	114 7(4)
C43-C41-O1	112 0(6)
C43-C41-C42	113 4(7)
O1 C41-C42	108 9(6)
O1-C44-C45	110 5(5)
O1-C44-C46	110 2(5)
C45-C44-C46	111 2(5)
C47-O2-C50	115 1(3)
C47 O2-Li	122 8(4)
C50 O2 Li	121 2(3)
O2-C47-C48	111 4(4)
O2 C47-C49	106 0(3)
C48-C47-C49	112.0(4)
O2-C50-C51	106 5(4)
O2 C50-C52	110 9(3)
C51-C50-C52	112 4(4)

Symmetry transformations used to generate equivalent atoms

Table 4 Anisotropic displacement parameters ($Å^2 \times 10^3$) for **2-6**. The anisotropic displacement factor exponent takes the form $-2\pi^2[h^2 a^{*2} U^{11} + \ldots + 2 h k a^* b^* U^{12}]$

	U^{11}	U^{22}	U^{33}	U^{23}	U^{13}	U^{12}
Zr	24(1)	32(1)	23(1)	1(1)	7(1)	1(1)
Cl1	40(1)	53(1)	28(1)	4(1)	4(1)	14(1)
Cl2	33(1)	48(1)	33(1)	0(1)	15(1)	-4(1)
B	23(2)	28(2)	26(2)	2(2)	8(2)	1(2)
Si	22(1)	36(1)	26(1)	0(1)	7(1)	2(1)
C15	30(2)	52(3)	33(2)	3(2)	9(2)	7(2)
C16	30(2)	51(3)	32(2)	-6(2)	6(2)	-2(2)
C1	45(3)	44(3)	42(3)	-13(2)	-4(2)	-2(2)
C2	50(3)	37(3)	49(3)	-12(2)	22(2)	-13(2)
C3	47(3)	30(2)	38(3)	1(2)	15(2)	0(2)
C4	42(2)	34(3)	38(2)	5(2)	19(2)	8(2)
C5	58(3)	37(3)	30(2)	-6(2)	13(2)	2(2)
C6	26(2)	38(2)	21(2)	-1(2)	10(2)	-1(2)
C7	27(2)	30(2)	25(2)	-4(2)	13(2)	-4(2)
C11	38(2)	32(3)	42(3)	0(2)	14(2)	-2(2)
C8	24(2)	47(3)	23(2)	-7(2)	10(2)	9(2)
C12	29(2)	58(3)	34(2)	9(2)	11(2)	-10(2)
C9	26(2)	42(3)	23(2)	-3(2)	5(2)	2(2)
C13	32(2)	57(3)	38(3)	1(2)	3(2)	4(2)
C10	24(2)	34(2)	23(2)	-1(2)	7(2)	0(2)
C14	36(2)	35(2)	28(2)	4(2)	9(2)	2(2)
C17	19(2)	30(2)	26(2)	7(2)	7(2)	4(2)
C18	23(2)	31(2)	27(2)	-4(2)	7(2)	2(2)
F1	39(1)	33(1)	36(1)	9(1)	17(1)	-5(1)
C19	20(2)	28(2)	28(2)	7(2)	7(2)	0(2)
F2	36(1)	25(1)	35(1)	2(1)	15(1)	-3(1)
C20	22(2)	25(2)	26(2)	3(2)	9(2)	4(2)
C21	28(2)	26(2)	28(2)	2(2)	6(2)	1(2)
F3	51(2)	25(1)	32(1)	-1(1)	15(1)	-5(1)

C22	26(2)	26(2)	31(2)	5(2)	10(2)	-1(2)
F4	56(2)	36(1)	36(1)	5(1)	21(1)	-13(1)
C23	27(2)	27(2)	21(2)	-1(2)	8(2)	4(2)
C24	34(2)	25(2)	29(2)	1(2)	12(2)	0(2)
F5	33(1)	31(1)	45(1)	10(1)	7(1)	3(1)
C25	29(2)	31(2)	28(2)	4(2)	6(2)	9(2)
F6	36(1)	44(2)	50(2)	11(1)	3(1)	14(1)
C26	21(2)	46(3)	29(2)	3(2)	7(2)	0(2)
F7	23(1)	61(2)	53(2)	5(1)	5(1)	1(1)
C27	30(2)	35(2)	33(2)	2(2)	10(2)	-6(2)
F8	31(1)	47(2)	63(2)	13(1)	12(1)	-10(1)
C28	30(2)	29(2)	26(2)	6(2)	10(2)	4(2)
F9	32(1)	33(1)	42(1)	14(1)	8(1)	0(1)
C29	33(2)	31(2)	22(2)	6(2)	6(2)	2(2)
C30	41(2)	32(2)	27(2)	7(2)	9(2)	3(2)
F10	30(1)	46(2)	48(2)	-1(1)	9(1)	-1(1)
C31	45(3)	41(3)	43(3)	2(2)	4(2)	-15(2)
F11	54(2)	64(2)	66(2)	-2(2)	1(1)	26(2)
C32	69(4)	32(3)	46(3)	-9(2)	5(3)	-14(3)
F12	102(3)	50(2)	77(2)	29(2)	15(2)	-27(2)
C33	61(3)	37(3)	47(3)	-11(2)	18(2)	2(2)
F13	93(2)	62(2)	89(2)	-37(2)	38(2)	3(2)
C34	39(2)	38(3)	36(2)	2(2)	12(2)	-2(2)
F14	44(2)	49(2)	54(2)	-14(1)	23(1)	1(1)
C35	26(2)	30(2)	26(2)	-1(2)	7(2)	-4(2)
C36	28(2)	32(2)	29(2)	3(2)	7(2)	2(2)
F15	39(1)	48(2)	30(1)	5(1)	16(1)	10(1)
C37	34(2)	37(2)	24(2)	6(2)	4(2)	-5(2)
F16	63(2)	57(2)	25(1)	13(1)	11(1)	3(1)
C38	38(2)	29(2)	30(2)	9(2)	8(2)	2(2)
F17	57(2)	52(2)	42(2)	18(1)	-2(1)	16(1)
C39	29(2)	38(3)	36(2)	3(2)	5(2)	8(2)
F18	44(2)	61(2)	56(2)	18(1)	13(1)	28(1)
C40	30(2)	32(2)	27(2)	8(2)	6(2)	2(2)
F19	33(1)	58(2)	37(1)	16(1)	17(1)	17(1)
Li	65(5)	38(5)	35(4)	7(3)	11(4)	-4(4)

O1	88(3)	40(2)	58(2)	0(2)	22(2)	12(2)
C41	114(6)	55(4)	99(5)	15(4)	63(5)	-8(4)
C42	227(10)	89(6)	96(6)	-45(5)	84(6)	-73(6)
C43	89(6)	88(6)	175(9)	20(5)	57(6)	12(5)
C44	76(4)	51(4)	66(4)	7(3)	9(3)	16(3)
C45	105(5)	112(6)	60(4)	3(4)	34(4)	21(4)
C46	78(5)	59(4)	121(6)	0(4)	5(4)	0(3)
O2	34(2)	42(2)	27(2)	1(1)	3(1)	5(1)
C47	39(3)	50(3)	36(3)	2(2)	1(2)	-1(2)
C48	43(3)	122(5)	32(3)	2(3)	3(2)	10(3)
C49	41(3)	59(3)	43(3)	3(2)	12(2)	1(2)
C50	39(2)	44(3)	33(2)	2(2)	10(2)	3(2)
C51	41(3)	60(4)	71(4)	9(3)	1(3)	1(3)
C52	56(3)	50(3)	55(3)	5(2)	24(3)	13(2)

Table 5 Hydrogen coordinates (x 10^4) and isotropic displacement parameters ($Å^2$x 10^3) for **2-6**

	x	y	z	U(eq)
H15A	6553	3438	12766	57
H15B	5157	3202	12373	57
H15C	5296	3417	13229	57
H16A	5448	4285	13309	56
H16B	5279	4536	12494	56
H16C	6650	4277	12804	56
H1A	3687	4617	14339	55
H2A	3249	4897	12899	52
H3A	578	4982	12371	45
H4A	-609	4739	13493	44
H5A	1298	4516	14705	49
H11A	1276	3065	12346	55
H11B	2869	3180	12731	55
H11C	2410	3055	11795	55
H12A	1083	3406	11017	59
H12B	-1694	3697	11590	59
H12C	844	3320	11971	59
H13A	-1195	4270	10580	64
H13B	334	4649	10947	64
H13C	-1315	4434	11450	64
H14A	2549	4558	10708	49
H14B	3481	4652	11595	49
H14C	1917	4817	11327	49
H41A	908	3037	13787	100
H42A	269	2563	12879	194
H42B	-1128	2688	13155	194
H42C	315	2302	13514	194

H43A	2452	2813	14932	170
H43B	2580	2549	14172	170
H43C	1720	2396	14812	170
H44A	592	2400	14814	78
H45A	428	2712	16035	135
H45B	-987	2492	16090	135
H45C	985	2953	15980	135
H46A	-2887	2928	14714	133
H46B	-2980	2472	14866	133
H46C	-2732	2628	14016	133
H47A	773	4224	16183	51
H48A	-491	3948	17083	100
H48B	1159	3905	17443	100
H48C	265	3541	17029	100
H49A	1807	3457	16052	71
H49B	2752	3818	16437	71
H49C	2039	3811	15485	71
H50A	-1918	4102	16051	46
H51A	-2843	3715	14533	89
H51B	-3873	3924	15014	89
H51C	-2991	3552	15398	89
H52A	-957	4571	15316	78
H52B	-2631	4567	15044	78
H52C	-1718	4367	14481	78

LIST OF REFERENCES

1 Silberberg, M *Chemistry The Molecular Nature of Matter and Change*, Mosby-Year Book Inc, St Louis, Missouri 1996

2. Marr, G , Rockett, B W *The Chemistry of the Metal-Carbon Bond*; John Wiley & Sons New York, 1982

3. Collman, J P , Hegedus L. S , Norton J. R , Finke, R. G *Principles and Applications of Organotransition Metal Chemistry*; University Science Books Mill Valley CA, 1987

4 Yamamoto, A. *Organotransition Metal Chemistry*, John Wiley & Sons New York, 1986

5 Wilkinson, G., Fauson, P L., Birmingham, J M., Cotton, F A *J Am Chem. Soc.* **1953** , *75*, 1011

6 Wilkinson, G *Noble Prize 1973*

7. Herrmann, W. A *Angewandte Chemie International Edition in English* **1982**, *21*, 117

8 Rofer-DePoorter, C K. *Chemical Reviews* **1981**, *81*, 447

9 Fischer, E. O *Advances in Organometallic Chemistry* **1976** *14*, 1

10 Fischer, E O *Noble Prize 1973*

11 Ziegler K., Holzkamp E , Breil, H , Martin H *Angewandte Chemie* **1955**, *67*, 541

12 Ziegler K. *Noble Prize 1963*

13 Natta, G *Angew Chem* **1956**, *68*, 393

14 Natta, G *Recieved the Noble Prize in 1963 for His Discoveries in the Field of the Chemistry and Technology of High Polymers*

15 Weissermel, K., Arpe, H -J *Industrial Organic Chemistry* 3rd ed. VCH: Weinheim, 1997

16 Bhadori S , Mukesh, D *Homogeneous Catalysis Mechanisms and Industrial Applications*, John Wiley & Sons, Inc New York 2000

17 Hagen, J *Industrial Catalysis a Practical Approach*, Wiley VCH. New York, 1999

18 Cotton, F A , Wilkinson, G *Advanced Inorgnic Chemistry*, John Wiley & Sons, Inc New York 1988

19 Crabtree, R H *The Organometallic Chemistry of the Transition Metals* John Wiley & Sons, Inc New York, 1994

20 Decker, S A., Cundari, T R. *Organometallics* **2001**, *20*(13), 2827-2841

21 Osborn, J A., Wilkinson, G , Young, J F *Chemical Communications* **1965**, (2), 17

22. Evans, D., Osborn, J A., Wilkinson G *Journal of the Chemical Society a - Inorganic Physical Theoretical* **1968** (12) 3133

23. Evans, D , Yagupsky, G , Wilkinson, G *Journal of the Chemical Society a - Inorganic Physical Theoretical* **1968**, (11) 2660

24 Brown, C K., Wilkinson, G. *Journal of the Chemical Society a Inorganic Physical Theoretical* **1970** (17), 2753

25 Yagupsky, G , Brown C K., Wilkinson, G *Journal of the Chemical Society a Inorganic Physical Theoretical* **1970**, (9) 1392

26 Robinson, A. J.; Lim, C. Y.; He, L. N.; Ma, P.; Li, H. Y. *Journal of Organic Chemistry* **2001**, *66*(12), 4141-4147

27 Bochmann, M. *Journal of the Chemical Society-Dalton Transactions* **1996**, (3), 255-270

28 Medermott, J. X.; White, J. F.; Whitesides, G. M. *Journal of the American Chemical Society* **1976**, *98*(21), 6521-6528

29 Angermund, K.; Fink, G.; Jensen, V. R.; Kleinschmidt, R. *Chemical Reviews* **2000**, *100*(4), 1457-1470

30 Alt, H. G.; Samuel, E. *Chemical Society Reviews* **1998**, *27*(5), 323-329

31 Alt, H. G.; Koppl, A. *Chemical Reviews* **2000**, *100*(4), 1205-1221

32 Tanke, R. S.; Crabtree, R. H. *Journal of the American Chemical Society* **1990**, *112*(22), 7984-7989

33 Benkeser, R. A.; Dunny, S.; Li, G. S.; Nerlekar, P. G.; Work, S. D. *Journal of the American Chemical Society* **1968**, *90*(7), 1871

34 Harrod, J. F.; Chalk, A. J. *Journal of the American Chemical Society* **1966**, *88*(15), 3491

35 Spetar, J. S. *Advances in Organometallic Chemistry* **1979**, *17*, 407

36 Casey, C. P.; Cyr, C. R. *Journal of the American Chemical Society* **1973**, *95*(7), 2240-2247

37 Casey, C. P.; Cyr, C. R. *Journal of the American Chemical Society* **1973**, *95*(7), 2248-2253

38 Parshall, G. W. *Homogeneous Catalysis: The Applications and Chemistry of Catalysis by Soluble Transition Metal Complexes* John Wiley & Sons, Inc.: New York, 1980

39 Parshall, G W *Journal of Molecular Catalysis* **1978**, *4*(4), 243-270

40 Tolman, C A., Mckinney, R J , Seidel, W C , Druliner, J D , Stevens, W R *Advances in Catalysis* **1985**, *33*, 1-46

41 Ziegler, K., Holzkamp, E., Breil, H Martin, H *Angewandte Chemie* **1955** *67*, 541

42 Natta, G *Angew Chem* **1956**, *68*, 393

43 Wilkinson, G., Birmingham, J M. *Journal of the American Chemical Society* **1954** *76*(17), 4281-4284

44 Birmingham, J M Seyferth D , Wilkinson G *Journal of the American Chemical Society* **1954** *76*(16), 4179

45 Wilkinson, G , Pauson, P L , Birmingham, J M., Cotton, F A *Journal of the American Chemical Society* **1953**, *75*(4), 1011-1012

46 Fischer, E. O *Angewandte Chemie* **1952** *22*, 620

47 Breslow, D S , Newberg, N R *Journal of the American Chemical Society* **1959**, *81*(1), 81

48 Breslow, D S , Newberg, N R *Journal of the American Chemical Society* **1957**, *79*(18), 5072

49 Bochmann, M *Journal of the Chemical Society-Dalton Transactions* **1996** (3), 255-270

50 Kaminsky, W *Journal of the Chemical Society, Dalton Transactions Inorganic Chemistry* **1998** 1413-1418

51 Mahrng, P C., Coville, N J *Journal of Organometallic Chemistry* **1994** *479* 1-29

52 Lanza, G., Fragala, I. L., Marks, T. J. *Journal of the American Chemical Society* **2000**, *122*(51), 12764-12777

53 Alt, H. G., Koppl, A. *Chemical Reviews* **2000**, *100*(4), 1205-1221

54 Angermund, K., Fink, G., Jensen, V. R., Kleinschmidt, R. *Chemical Reviews* **2000**, *100*(4), 1457-1470

55 Sinn, H., Kaminsky, W., Vollmer, H. J., Woldt, R. *Angewandte Chemie International Edition in English* **1980**, *19*(5), 390-392

56 Kaminsky, W., Miri, M., Sinn, H., Woldt, R. *Makromolekulare Chemie-Rapid Communications* **1983**, *4*(6), 417-421

57 Cihlar, J., Mejzlik, J., Hamrik, O., Hudec, P., Majer, J. *Makromolekulare Chemie-Macromolecular Chemistry and Physics* **1980**, *181*(12), 2549-2561

58 Mason, M. R., Smith, J. M., Bott, S. G., Barron, A. R. *Journal of the American Chemical Society* **1993**, *115*(12), 4971-4984

59 Zurek, E., Ziegler, T. *Inorganic Chemistry* **2001**, *40*(14), 3279-3292

60 Collman, J. P., Hegedus, L. S., Norton, J. R., Finke, R. G. *Principles and Applications of Organotransition Metal Chemistry*; University Science Books: Mill Valley, CA, 1987

61 Cossee, P. *Journal of Catalysis* **1964**, *3*(1), 80-88

62 Arlman, E. J., Cossee, P. *Journal of Catalysis* **1964**, *3*(1), 99-104

63 Ivin, K. J., Rooney, J. J., Stewart, C. D., Green, M. L. H., Mahtab, R. *Journal of the Chemical Society-Chemical Communications* **1978**, (14), 604-606

64 Sinn, H., Kaminsky, W. *Advances in Organometallic Chemistry* **1980**, *18*, 99

65 Kissin, Y. V., Brandolini, A. J. *Journal of Polymer Science Part a-Polymer*

Chemistry **1999**, *37*(23) 4273-4280

66 Bhaduri, S ; Mukesh, D *Homogeneous Catalysis Mechanisms and Industrial Applications*, John Wiley & Sons, Inc New York, 2000

67 Parshall, G W *Homogeneous Catalysis The Applications and Chemistry of Catalysis by Soluble Transition Metal Complexes* John Wiley & Sons, Inc New York, 1980

68 Crabtree, R H *The Organometallic Chemistry of the Transition Metals*, John Wiley & Sons Inc New York, 1994

69 Keim, W , Schulz, R. P *Journal of Molecular Catalysis* **1994**, *92*(1), 21 33

70 Keim, W *Angewandte Chemie International Edition in English* **1990** *29*(3), 235-244

71 Killian, C M., Tempel D J , Johnson, L K , Brookhart, M *Journal of the American Chemical Society* **1996** *118*(46), 11664-11665

72 Johnson L K , Mecking, S , Brookhart, M *Journal of the American Chemical Society* **1996** *118*(1), 267-268

73 Johnson, L K , Killian C M , Brookhart, M *Journal of the American Chemical Society* **1995** *117*(23), 6414-6415

74 Abeywickrema, R , Bennett, M A , Cavell, K J , Kony, M , Masters, A F , Webb, A G *Journal of the Chemical Society-Dalton Transactions* **1993** (1), 59-68

75 Brown, S J , Masters, A F *Journal of Organometallic Chemistry* **1989**, *367*(3), 371-374

76 Hoveyda, A H , Morken, J P *Angewandte Chemie International Edition in English* **1996**, *35*(12), 1262-1284

77 Christ, C. S., Eyler, J. R., Richardson, D. E. *Journal of the American Chemical Society* **1990**, *112*, 4778

78 Christ, C. S.; Eyler, J. R., Richardson, D. E. *Journal of the American Chemical Society* **1990**, *112*, 596

79 Christ, C. S.; Eyler, J. R., Richardson, D. E. *Journal of the American Chemical Society* **1998**, *110*, 4038

80 Richardson, D. E.; Ryan, M. F.; Khan, M. N. I., Maxwell, K. A. *Journal of the American Chemical Society* **1992**, *114*, 10482.

81 Richardson, D. E., Alameddin, N. G., Ryan, M. F., Hayes, T., Eyler, J. R., Siedle, A. R. *J. Am. Chem. Soc.* **1996**, *118*(45), 11244-11253

82 Jordan, R. F. *Advances in Organometallic Chemistry* **1991**, *32*, 325-387

83 Jordan, R. F., Bajgur, C. S., Willett, R., Scott, B. *Journal of the American Chemical Society* **1986**, *108*(23), 7410-7411

84 Hlatky, G. G., Turner, H. W., Eckman, R. R. *Journal of the American Chemical Society* **1989**, *111*(7), 2728-2729

85 Bochmann, M., Jaggar, A. J., Nicholls, J. C. *Angewandte Chemie International Edition in English* **1990**, *29*(7), 780-782

86 Horton, A. D., Frijns, J. H. G. *Angewandte Chemie-International Edition in English* **1991**, *30*(9), 1152-1154

87 Piers, W. E., Chivers, T. *Chemical Society Reviews* **1997**, *26*(5), 345-354

88 Massey, A. G., Park, A. J. *Journal of Organometallic Chemistry* **1966**, *5*(3), 218

89 Massey, A. G., Park, A. J. *Journal of Organometallic Chemistry* **1964**, *2*(3), 245-250

90 Yang, X. M.; Stern, C. L.; Marks, T. J. *Journal of the American Chemical Society* **1994**, *116*(22), 10015-10031.

91 Yang, X. M.; Stern, C. L.; Marks, T. J. *Journal of the American Chemical Society* **1991**, *113*(9), 3623-3625.

92. Chen, Y. X.; Stern, C. L.; Yang, S. T.; Marks, T. J. *Journal of the American Chemical Society* **1996**, *118*(49), 12451-12452.

93 Li, L. T.; Marks, T. J. *Organometallics* **1998**, *17*(18), 3996-4003.

94 Li, L. T.; Stern, C. L.; Marks, T. J. *Organometallics* **2000**, *19*(17), 3332-3337.

95 Metz, M. V.; Schwartz, D. J.; Stern, C. L.; Nickias, P. N.; Marks, T. J. *Angewandte Chemie International Edition* **2000**, *39*(7), 1312-+.

96 Lee, L. W. M.; Piers, W. E.; Parvez, M.; Rettig, S. J.; Young, V. G. *Organometallics* **1999**, *18*(19), 3904-3912.

97 Williams, V. C.; Dai, C. Y.; Li, Z. M.; Collins, S.; Piers, W. E.; Clegg, W.; Elsegood, M. R. J.; Marder, T. B. *Angewandte Chemie International Edition* **1999**, *38*(24), 3695-3698.

98 Temme, B.; Erker, G.; Karl, J.; Luftmann, H.; Frohlich, R.; Kotila, S. *Angew. Chem. Int. Ed. Engl.* **1995**, *34*(16), 1755-1757.

99 Temme, B.; Erker, G.; Karl, J.; Luftmann, H.; Frohlich, R.; Kotila, S. *Angewandte Chemie-International Edition in English* **1995**, *34*(16), 1755-1757.

100 Bochmann, M.; Lancaster, S. J.; Robinson, O. B. *Journal of the Chemical Society-Chemical Communications* **1995**, (20), 2081-2082.

101 Ruwwe, J.; Erker, G.; Frohlich, R. *Angewandte Chemie-International Edition in English* **1996**, *35*(1), 80-82.

102 Sun, Y.; Spence, R. E.; Piers, W. E.; Parvez, M.; Yap, G. P. A. *J. Am. Chem. Soc.* **1997**, *119*(22), 5132-5143.

103 Song, X. J.; Bochmann, M. *Journal of Organometallic Chemistry* **1997**, *546*, 597-600

104 Coates, G. E.; Green, M. L. H.; Wade, K. *Organometallic Compounds. The Main Group Elements*; 3rd ed.; Methuen & Co.: London, 1967

105 Shafiq, F. A.; Abboud, K. A.; Richardson, D. E.; Boncella, J. M. *Organometallics* **1998**, *17*(5), 982-985

106 Sun, Y. M.; Spence, Revh.; Piers, W. E.; Parvez, M.; Yap, G. P. A. *Journal of the American Chemical Society* **1997**, *119*(22), 5132-5143

107 Shapiro, P. J.; Cotter, W. D.; Schaefer, W. P.; Labinger, J. A.; Bercaw, J. E. *J. Am. Chem. Soc.* **1994**, *116*(11), 4623-4640

108 Ewen, J. A.; Elder, M. J. European Patent 154-730

109 Lund, E. C.; Livinghouse, T. *Organometallics* **1990**, *9*(9), 2426-2427

110 Chen, E. Y. X.; Marks, T. J. *Chemical Reviews* **2000**, *100*(4), 1391-1434

111 Cotton, F. A.; Wilkinson, G. *Advanced Inorganic Chemistry*; John Wiley & Sons, Inc.: New York, 1988

112 Jia, L.; Yang, X. M.; Ishihara, A.; Marks, T. J. *Organometallics* **1995**, *14*(7), 3135-3137

113 Schrock, R. R.; Casado, A. L.; Goodman, J. T.; Liang, L. C.; Bonitatebus, P. J.; Davis, W. M. *Organometallics* **2000**, *19*(25), 5325-5341

114 Thayer, A. M. *Chemical & Engineering News* **1996**, *74*(25), 15-17

115 Alt, H. G.; Koppl, A. *Chemical Reviews* **2000**, *100*(4), 1205-1221

116 Johnson, L. K.; Killian, C. M.; Brookhart, M. *Journal of the American Chemical Society* **1995**, *117*(23), 6414-6415

117 Johnson, L. K., Mecking, S., Brookhart, M. *Journal of the American Chemical Society* **1996**, *118*(1), 267-268

118 Killian, C. M., Tempel, D. J., Johnson, L. K., Brookhart, M. *Journal of the American Chemical Society* **1996**, *118*(46), 11664-11665

119 Carpenetti, D. W., Kloppenburg, L., Kupec, J. T., Petersen, J. L. *Organometallics* **1996**, *15*(11), 2668

120 Sinnema, P. J., Liekelema, K., Staal, O. K. B., Hessen, B., Teuben, J. H. *Journal of Molecular Catalysis a Chemical* **1998**, *128*(1-3), 143-153

121 Shapiro, P. J., Bunel, E., Schaefer, W. P., Bercaw, J. E. *Organometallics* **1990**, *9*(3), 867-869

122 Shapiro, P. J., Cotter, W. D., Schaefer, W. P., Labinger, J. A., Bercaw, J. E. *Journal of the American Chemical Society* **1994**, *116*(11), 4623-4640

123 Canich, J. A. M. 5,026,798, June 25, 1991

124 Stevens, J. C., Timmers, F. J., Wilson, D. R., Schmidt, G. F., Nickias, P. N., Rosen, R. K., Knight, G. W., Lai, S. Europe EP-416-815-A2

125 Hughes, A. K., Meetsma, A., Teuben, J. H. *Organometallics* **1993**, *12*(5), 1936-1945

126. Fandos, R., Meetsma, A., Teuben, J. H. *Organometallics* **1991**, *10*(1), 59-60

127 Carpenetti, D. W., Kloppenburg, L., Kupec, J. T., Petersen, J. L. *Organometallics* **1996**, *15*(6), 1572-1581

128 Kloppenburg, L., Petersen, J. L. *Organometallics* **1997**, *16* (15), 3548-3556

129 Galan Fereres, M., Koch, T., Hey-Hawkins, E., Eisen, M. *Journal of Organometallic Chemistry* **1999**, *580*, 145-155

130 Jia, L , Yang, X M , Stern, C L , Marks, T J *Organometallics* **1997**, *16*(5), 842-857

131 Chen, Y X , Stern, C L., Yang, S T., Marks, T J *Journal of the American Chemical Society* **1996** *118*(49), 12451-12452.

132. Small, B L., Brookhart, M *Journal of the American Chemical Society* **1998** *120*(28), 7143-7144

133 Small, B L., Brookhart, M. *Macromolecules* **1999**, *32*(7) 2120-2130

134 Small, B L., Brookhart, M , Bennett, A M. A *Journal of the American Chemical Society* **1998**, *120*(16) 4049-4050

135 Rix, F , Brookhart, M. *Journal of the American Chemical Society* **1995**, *117*, 1137-1138

136 Miller, H J University of Florida, 1997

137 Walton, D R. M *Journal of the Chemical Society C-Organic* **1966**, (19), 1706-&.

138 Greene, T W., Wuts, P G M *Protective Groups in Organic Synthesis*, John Wiley & Sons, Inc., New York 1991.

139 Schnzer, D , Heathcock, C H *Tetrahedron Letters* **1981**, *22*(20), 1883-1884

140 Hosomi, A., Shirahata, A., Sakurai, H *Tetrahedron Letters* **1978** (33) 3043-3046

141 Nakamura, E , Shimizu, M., Kuwajima, I *Tetrahedron Letters* **1976** (20), 1699-1702.

142 Belsky, I *Journal of the Chemical Society-Chemical Communications* **1977**, (7), 237237

143 Brook, A G., Duff, J M., Nones, P. F , Davis, N R. *Journal of the American*

Chemical Society, **1967**, *89*(2), 431-&.

144 Jones, M. *Organic Chemistry*, W.W. Norton & Company: New York, 1997.

145 Taguchi, K., Westheimer, F.H. *Journal of Organic Chemistry* **1971**, *36*(11), 1570-&.

146 Layer, R.W. *Chemical Reviews* **1963**, *63*(5), 489-&.

147 Shapiro, P.J., Cotter, W.D., Schaefer, W.P., Labinger, J.A., Bercaw, J.E. *J. Am. Chem. Soc.* **1994**, *116*(11), 4623-4640.

148 Okuda, J., Schattenmann, F.J., Wocadlo, S., Massa, W. *Organometallics* **1995**, *14*(2), 789-795.

149 Okuda, J. *Chemische Berichte* **1990**, *123*(8), 1649-1651.

150 Chandra, G., Lappert, M.F. *Journal of the Chemical Society a - Inorganic Physical Theoretical* **1968**, (8), 1940.

151 Sheldon, R.A., Kochi, J.K. *Metal-Catalyzed Oxidations of Organic Compounds*; Academic press: New York, 1981.

152 March, J. *Advanced Organic Chemistry*, Fourth ed. John Wiley & Sons, New York, 1992.

153 Suresh, A.K., Sridhar, T., Potter, O.E. *Aiche Journal* **1988**, *34*(1), 69-80.

154 Wen, Y., Potter, O.E., Sridhar, T. *Chemical Engineering Science* **1997**, *52*(24), 4593-4605.

155 Bhaduri, S.; Mukesh, D. *Homogeneous Catalysis: Mechanisms and Industrial Applications*, John Wiley & Sons, Inc.: New York, 2000.

156 Sheldon, R. A., Vandoorn J. A. *Journal of Catalysis* **1974**, *34*(2), 242-245.

157 Sheldon, R. A., Vandoorn, J. A. *Journal of Catalysis* **1973**, *31*(3), 427-437

158 Sheldon, R. A., Vandoorn J. A., Schram, C. W. A., Dejong, A. J. *Journal of Catalysis* **1973**, *31*(3), 438-443

159 Sheldon, R. A. *Recueil Des Travaux Chimiques Des Pays-Bas-Journal of the Royal Netherlands Chemical Society* **1973**, *92*(3), 367-373

160 Sheng, M. N., Zajacek J. G. *Journal of Organic Chemistry* **1970**, *35*(6), 1839-&

161 *Chemical Week* **March 10, 1999**, 31

162 Castellan, A., Bart, J. C. J., Cavallaro, S. *Catalysis Today* **1991**, *9*(3), 255-283

163 Castellan, A., Bart, J. C. J., Cavallaro, S. *Catalysis Today* **1991**, *9*(3), 237-254

164 Thiemens, M. H., Trogler, W. C. *Science* **1991**, *251*(4996), 932-934

165 Schuchardt, U., Cardoso, D., Sercheli, R., Pereira, R., De Cruz, R. S., Guerreiro, M. C., Mandelli, D., Spinace, E. V., Fires, E. L. *Applied Catalysis a - Chemical* **2001**, *211*(1), 1-17.

166 Dugal, M., Sankar, G., Raja, R., Thomas, J. M. *Angewandte Chemie International Edition* **2000**, *39*(13), 2310-2313

167 Thomas, J. M., Raja, R., Sankar, G., Bell, R. G. *Accounts of Chemical Research* **2001**, *34*(3), 191-200

168 Chen, J. D., Sheldon, R. A. *Journal of Catalysis* **1995**, *153*(1), 1-8

169 Raja, R., Sankar, G., Thomas, J. M. *Angewandte Chemie-International Edition* **2000**, *39*(13), 2313-2316

170 Tanaka, K. *Chem Tech* **1974**, 555.

171 Park, C.-M.; Goroff, N. S. United States 5,221,800, June 22, 1993

172 Reimer, R. A.; Slaten, C. S.; Seapan, M.; Koch, T. A.; Triner, V. G. *"Adipic Acid Industry--N2O Abatement" Non CO2 Greenhouse Gases: Scientific Understanding, Control and Implementation*, Kluwer Academic Publishers: New York, 2000

173 Goldstein, A. S.; Beer, R. H.; Drago, R. S. *Journal of the American Chemical Society* **1994**, *116*(6), 2424-2429

174 Cheng Xu University of Florida, PhD 1999

175 Labinger, J. A. *Catalysis Letters* **1994**, *26*(1-2), 95-99

176 Lyons, J. E., Ellis, P. E., Myers, H. K. *Journal of Catalysis* **1995**, *155*(1), 59-73

177 Bottcher, A.; Birnbaum, E. R.; Day, M. W.; Gray, H. B.; Grinstaff, M. W.; Labinger, J. A. *Journal of Molecular Catalysis a-Chemical* **1997**, *117*(1-3), 229-242

178 Lyons, J. E., Ellis, P. E. Myers, H. K., Wagner, R. W. *Journal of Catalysis* **1993**, *141*(1), 311-315

179 Sheldon, R. A., Kochi, J. K. *Metal Catalyzed Oxidations of Organic Compounds* Academic press: New York, 1981

180 Tolman, C. A.; Druliner, J. D.; Nappa, M. J.; Herron, N. *Activation and Functionalization of Alkanes*, John Wiley & Sons: New York, 1989

181 Castellan, A., Bart, J. C. J., Cavallaro, S. *Catalysis Today* **1991**, *9*(3), 255-283

182 Barton, D. H. R. *Journal of Molecular Catalysis a-Chemical* **1997**, *117*(1-3), 3-7

183 Barton, D. H. R. *Tetrahedron* **1998**, *54*(22), 5805-5817

184 Barton, D. H. R., Chabot, B. M. *Tetrahedron* **1997**, *53*(2), 487-510

185 Barton, D. H. R.; Baviere, S. D.; Hill, D. R. *Tetrahedron* **1994**, *50*(9), 2665-2670

186 Barton, D. H. R.; Beck, A. H.; Delanghe, N. C. *Tetrahedron Letters* **1996**, *37*(10), 1555-1558

187 Bardin, C.; Barton, D. H. R.; Hu, B.; Rojas-Wahl, R.; Taylor, D. K. *Tetrahedron Letters* **1994**, *35*, 5805-5808

188 Baron, D. H. R.; Doller, D. *Acc. Chem. Res.* **1992**, *25*, 504-512

189 Barton, D. H. R.; Chabot, B. M.; Delanghe, N. C.; Hu, B.; Le Gloahec, V. N.; Rojas-Wahl, R. U. *Tetrahedron Letters* **1995**, *36*, 7007-7010

190 Barton, D. H. R.; Halley, F.; Ozbalik, N.; Schmitt, M.; Young, E.; Balavoine, G. *Journal of the American Chemical Society* **1989**, *111*, 7144-7149

191 Barton, D. H. R.; Chabot, B. M.; Hu, B. *Tetrahedron* **1996**, *52*(31), 10301-10312

BIOGRAPHICAL SKETCH

Garry Kenneth Weakley was born in Clarksville, Tennessee, on December 22, 1970 to Garry and Judy Weakley He lived in Clarksville, Tennessee throughout his formative years Garry graduated from Clarksville High School in Clarksville Tennessee during the spring of 1989. In the fall of that year he decided to attend Austin Peay State University where he initiated studies in chemistry and math Under the guidance of Dr Lori Slavin he sought to pursue a graduate degree in chemistry Graduating from Austin Peay in December of 1995 with a B S in chemistry, Garry chose to pursue his graduate degree at the University of Florida At the University of Florida Garry joined the research group of Dr David Richardson, where he earned his Ph. D in Inorganic Chemistry Upon graduation Garry will pursue a career as an organic chemist at CB Research and Development in New Castle, Delaware

I certify that I have read this study and that in my opinion it conforms to acceptable standards of scholarly presentation and is fully adequate, in scope and quality, as a dissertation for the degree of Doctor of Philosophy

David E. Richardson, Chair
Professor of Chemistry

I certify that I have read this study and that in my opinion it conforms to acceptable standards of scholarly presentation and is fully adequate, in scope and quality, as a dissertation for the degree of Doctor of Philosophy

James M. Boncella
Professor of Chemistry

I certify that I have read this study and that in my opinion it conforms to acceptable standards of scholarly presentation and is fully adequate, in scope and quality, as a dissertation for the degree of Doctor of Philosophy

Gus J. Palenik
Professor of Chemistry

I certify that I have read this study and that in my opinion it conforms to acceptable standards of scholarly presentation and is fully adequate, in scope and quality, as a dissertation for the degree of Doctor of Philosophy

Kirk S. Schanze
Professor of Chemistry

I certify that I have read this study and that in my opinion it conforms to acceptable standards of scholarly presentation and is fully adequate, in scope and quality, as a dissertation for the degree of Doctor of Philosophy

Robert M. Pigg, Jr.
Professor of Health and Science Education

This dissertation was submitted to the Graduate Faculty of the Department of Chemistry in the College of Liberal Arts and Sciences and to the Graduate School and was accepted as partial fulfillment of the requirements for the degree of Doctor of Philosophy

May, 2003

Dean, Graduate School